2. Two-Level Atoms and Spontaneous Emission

The damped harmonic oscillator provides our elementary description for the electromagnetic field in a lossy cavity. The damped two-level atom will provide our elementary description for the matter with which this field interacts. In an atomic vapor, loss of energy from an excited atom may take place via spontaneous emission or inelastic collisions. Elastic collisions can also play an important damping role; although, of course, they do not carry away energy; elastic collisions interrupt the phase of induced electronic oscillations and in this way damp the atomic polarization. We will first restrict our treatment to the case of purely radiative damping, assuming conditions in which collisions are unimportant. Such conditions are achieved, for example, in atomic beams. Later we will derive the terms that must be added to the master equation to describe additional phase destroying processes such as elastic collisions.

We consider an atom with two states, designated $|1\rangle$ and $|2\rangle$, having energies E_1 and E_2 with $E_1 < E_2$. Radiative transitions between $|1\rangle$ and $|2\rangle$ are allowed in the dipole approximation. Our objective is to describe energy dissipation and polarization damping through the coupling of the $|1\rangle \rightarrow |2\rangle$ transition to the many modes of the vacuum radiation field (a reservoir of harmonic oscillators). For simplicity we assume that there are no transitions between $|1\rangle$ and $|2\rangle$ and any other states of the atom. The extension to multilevel atoms can be found in Louisell [2.1] and Haken [2.2]. A treatment for just two levels which corresponds closely to our own is given in Sargent, Scully and Lamb [2.3].

2.1 Two-Level Atom as a Pseudo-Spin System

A two-state system can be described in terms of the Pauli spin operators. We will be using this description extensively and we therefore begin by briefly reviewing the relationship between these operators and quantities of physical interest, such as the atomic inversion and polarization. A more complete coverage of this subject is given by Allen and Eberly [2.4].

If we have a representation in terms of a complete set of states $|n\rangle, n = 1, 2, \ldots$, any operator $\hat{O}$ can be expanded as

$$\hat{O} = \sum_{n,m} \langle n|\hat{O}|m\rangle |n\rangle\langle m|. \tag{2.1}$$

This follows after multiplying on the left and right by the identity operator $\hat{I} = \sum_n |n\rangle\langle n|$. The $\langle n|\hat{O}|m\rangle$ define the matrix representation of $\hat{O}$ with respect to the basis $|n\rangle$. If we adopt the energy eigenstates $|1\rangle$ and $|2\rangle$ as a basis for our two-level atom, the unperturbed atomic Hamiltonian H_A can then be written in the form

$$\begin{aligned} H_A &= E_1|1\rangle\langle 1| + E_2|2\rangle\langle 2| \\ &= \tfrac{1}{2}(E_1 + E_2)\hat{I} + \tfrac{1}{2}(E_2 - E_1)\sigma_z, \end{aligned} \tag{2.2}$$

where

$$\sigma_z \equiv |2\rangle\langle 2| - |1\rangle\langle 1|. \tag{2.3}$$

The first term in (2.2) is a constant which may be eliminated by referring the atomic energies to the middle of the atomic transition, as in Fig. 2.1. We then write

$$H_A = \tfrac{1}{2}\hbar\omega_A\sigma_z, \qquad \omega_A \equiv (E_2 - E_1)/\hbar. \tag{2.4}$$

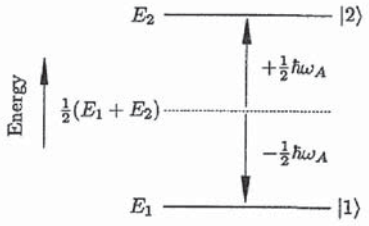

Fig. 2.1 Energy levels for a two-level atom.

Consider now the dipole moment operator $e\hat{\boldsymbol{q}}$, where e is the electronic charge and $\hat{\boldsymbol{q}}$ is the coordinate operator for the bound electron:

$$\begin{aligned} e\hat{\boldsymbol{q}} &= e\sum_{n,m=1}^{2} \langle n|\hat{\boldsymbol{q}}|m\rangle |n\rangle\langle m| \\ &= e\big(\langle 1|\hat{\boldsymbol{q}}|2\rangle |1\rangle\langle 2| + \langle 2|\hat{\boldsymbol{q}}|1\rangle |2\rangle\langle 1|\big) \\ &= \boldsymbol{d}_{12}\sigma_- + \boldsymbol{d}_{21}\sigma_+, \end{aligned} \tag{2.5}$$

where we have set $\langle 1|\hat{\boldsymbol{q}}|1\rangle = \langle 2|\hat{\boldsymbol{q}}|2\rangle = 0$, assuming atomic states whose symmetry guarantees zero permanent dipole moment, and we have introduced the *atomic dipole matrix elements*

$$\boldsymbol{d}_{12} \equiv e\langle 1|\hat{\boldsymbol{q}}|2\rangle, \qquad \boldsymbol{d}_{21} = (\boldsymbol{d}_{12})^*, \tag{2.6}$$

and *atomic lowering and raising operators*

$$\sigma_- \equiv |1\rangle\langle 2|, \qquad \sigma_+ \equiv |2\rangle\langle 1|. \tag{2.7}$$

The matrix representations for the operators introduced in (2.3) and (2.7) are

$$\sigma_z = \begin{pmatrix} 1 & 0 \\ 0 & -1 \end{pmatrix}, \qquad \sigma_- = \begin{pmatrix} 0 & 0 \\ 1 & 0 \end{pmatrix}, \qquad \sigma_+ = \begin{pmatrix} 0 & 1 \\ 0 & 0 \end{pmatrix}. \tag{2.8}$$

By writing

$$\sigma_\pm = \tfrac{1}{2}(\sigma_x \pm i\sigma_y), \tag{2.9}$$

with

$$\sigma_x = \begin{pmatrix} 0 & 1 \\ 1 & 0 \end{pmatrix}, \qquad \sigma_y = \begin{pmatrix} 0 & -i \\ i & 0 \end{pmatrix}, \tag{2.10}$$

we see that σ_x, σ_y, and σ_z are the *Pauli spin matrices* introduced initially in the context of magnetic transitions in spin-$\frac{1}{2}$ systems [2.5]. When applied to two-level atoms σ_z, σ_-, and σ_+ are referred to as *pseudo-spin operators*, since, in this context the two levels are not associated with the states of a real spin.

Exercise 2.1 From the relationships above, deduce the following:

1. the commutation relations

$$[\sigma_+, \sigma_-] = \sigma_z, \qquad [\sigma_\pm, \sigma_z] = \mp 2\sigma_\pm; \tag{2.11}$$

2. the action on atomic states:

$$\sigma_z|1\rangle = -|1\rangle, \qquad \sigma_z|2\rangle = |2\rangle, \tag{2.12a}$$
$$\sigma_-|1\rangle = 0, \qquad \sigma_-|2\rangle = |1\rangle, \tag{2.12b}$$
$$\sigma_+|1\rangle = |2\rangle, \qquad \sigma_+|2\rangle = 0. \tag{2.12c}$$

From (2.12b) and (2.12c) the designation of σ_- and σ_+ as atomic lowering and raising operators is clear.

We will formulate our description of two-level atoms in terms of the operators σ_z, σ_-, and σ_+. For an atomic state specified by a density operator ρ, expectation values of σ_z, σ_-, and σ_+ are just the matrix elements of the density operator, and give the *population difference*

$$\langle \sigma_z \rangle = \mathrm{tr}(\rho\sigma_z) = \langle 2|\rho|2\rangle - \langle 1|\rho|1\rangle = \rho_{22} - \rho_{11}, \tag{2.13}$$

and the mean *atomic polarization*

$$\begin{aligned} \langle e\hat{\boldsymbol{q}} \rangle &= \boldsymbol{d}_{12}\mathrm{tr}(\rho\sigma_-) + \boldsymbol{d}_{21}\mathrm{tr}(\rho\sigma_+) \\ &= \boldsymbol{d}_{12}\langle 2|\rho|1\rangle + \boldsymbol{d}_{21}\langle 1|\rho|2\rangle \\ &= \boldsymbol{d}_{12}\,\rho_{21} + \boldsymbol{d}_{21}\,\rho_{12}. \end{aligned} \tag{2.14}$$

2.2 Spontaneous Emission in the Master Equation Approach

2.2.1 Master Equation for a Radiatively Damped Two-Level Atom

We consider an atom that is radiatively damped by its interaction with the many modes of the radiation field taken in thermal equilibrium at temperature T. This field acts as a reservoir of harmonic oscillators. Within the general formula for a system S interacting with a reservoir R, the Hamiltonian (1.16) is given in the rotating-wave and dipole approximations by [2.6, 2.7]

$$H_S \equiv \tfrac{1}{2}\hbar\omega_A\sigma_z, \tag{2.15a}$$
$$H_R \equiv \sum_{k,\lambda} \hbar\omega_k r^\dagger_{k,\lambda} r_{k,\lambda}, \tag{2.15b}$$
$$H_{SR} \equiv \sum_{k,\lambda} \hbar\left(\kappa^*_{k,\lambda} r^\dagger_{k,\lambda}\sigma_- + \kappa_{k,\lambda} r_{k,\lambda}\sigma_+\right), \tag{2.15c}$$

with

$$\kappa_{k,\lambda} \equiv -ie^{i\boldsymbol{k}\cdot\boldsymbol{r}_A}\sqrt{\frac{\omega_k}{2\hbar\epsilon_0 V}}\,\hat{e}_{k,\lambda}\cdot\boldsymbol{d}_{21}. \tag{2.16}$$

The summation extends over reservoir oscillators (modes of the electromagnetic field) with wavevectors $\boldsymbol{k}$ and polarization states λ, and corresponding frequencies ω_k and unit polarization vectors $\hat{e}_{k,\lambda}$. The atom is positioned at $\boldsymbol{r}_A$, and V is the quantization volume. $\kappa_{k,\lambda}$ is the *dipole coupling constant* for the electromagnetic field mode with wavevector $\boldsymbol{k}$ and polarization λ. The general formalism from Sect. 1.3 now takes us directly to (1.34), where from (1.32) and (2.15) we must make the identification:

$$s_1 = \sigma_-, \qquad s_2 = \sigma_+, \tag{2.17a}$$
$$\Gamma_1 = \Gamma^\dagger \equiv \sum_{k,\lambda} \kappa^*_{k,\lambda} r^\dagger_{k,\lambda}, \qquad \Gamma_2 = \Gamma \equiv \sum_{k,\lambda} \kappa_{k,\lambda} r_{k,\lambda}. \tag{2.17b}$$

In the interaction picture,

$$\tilde{\Gamma}_1(t) = \tilde{\Gamma}^\dagger(t) = \sum_{k,\lambda} \kappa^*_{k,\lambda} r^\dagger_{k,\lambda} e^{i\omega_k t}, \tag{2.18a}$$
$$\tilde{\Gamma}_2(t) = \tilde{\Gamma}(t) = \sum_{k,\lambda} \kappa_{k,\lambda} r_{k,\lambda} e^{-i\omega_k t}, \tag{2.18b}$$

and

$$\tilde{s}_1(t) = e^{i(\omega_A\sigma_z/2)t}\sigma_- e^{-i(\omega_A\sigma_z/2)t} = \sigma_- e^{-i\omega_A t}, \tag{2.19a}$$
$$\tilde{s}_2(t) = e^{i(\omega_A\sigma_z/2)t}\sigma_+ e^{-i(\omega_A\sigma_z/2)t} = \sigma_+ e^{i\omega_A}. \tag{2.19b}$$

Note 2.1 To obtain (2.19), consider the Heisenberg equation of motion

$$\begin{aligned}\dot{\tilde{s}}_1 &= i\tfrac{1}{2}\omega_A e^{i(\omega_A\sigma_z/2)t}(\sigma_z\sigma_- - \sigma_-\sigma_z)e^{-i(\omega_A\sigma_z/2)t}\\ &= -i\omega_A\tilde{s}_1.\end{aligned}$$

This is trivially solved to give

$$\tilde{s}_1(t) = \tilde{s}_1(0)e^{-i\omega_A t} = \sigma_- e^{-i\omega_A t}.$$

Aside from the obvious notational differences, (2.18) and (2.19) are the same as (1.41) and (1.40), respectively, with the substitution $a \to \sigma_-$, $a^\dagger \to \sigma_+$. The derivation of the master equation for a two-level atom then follows in complete analogy to the derivation of the master equation for the harmonic oscillator, aside from two minor differences: (1) The explicit evaluation of the summation over reservoir oscillators now involves a summation over wavevector directions and polarization states. (2) The commutation relations used to reduce the master equation to its simplest form are different. Neither of these steps are taken in passing from (1.34) to (1.62), or in evaluating the time integrals using (1.65). We can therefore simply make the substitution $a \to \sigma_-$, $a^\dagger \to \sigma_+$ in (1.62) to write

$$\begin{aligned}\dot{\tilde{\rho}} = &\left[\frac{\gamma}{2}(\bar{n}+1) + i(\Delta'+\Delta)\right](\sigma_-\tilde{\rho}\sigma_+ - \sigma_+\sigma_-\tilde{\rho})\\ &+ \left(\frac{\gamma}{2}\bar{n} + i\Delta'\right)(\sigma_+\tilde{\rho}\sigma_- - \tilde{\rho}\sigma_-\sigma_+) + \text{h.c.},\end{aligned} \tag{2.20}$$

with $\bar{n} \equiv \bar{n}(\omega_A, T)$ and

$$\gamma \equiv 2\pi\sum_\lambda \int d^3k\, g(\boldsymbol{k})|\kappa(\boldsymbol{k},\lambda)|^2\delta(kc-\omega_A), \tag{2.21}$$

$$\Delta \equiv \sum_\lambda P\int d^3k\, \frac{g(\boldsymbol{k})|\kappa(\boldsymbol{k},\lambda)|^2}{\omega_A - kc}, \tag{2.22}$$

$$\Delta' \equiv \sum_\lambda P\int d^3k\, \frac{g(\boldsymbol{k})|\kappa(\boldsymbol{k},\lambda)|^2}{\omega_A - kc}\bar{n}(kc,T). \tag{2.23}$$

We have grouped the terms slightly differently in (2.20), but the correspondence to (1.62) is clear when we note that, there, $\alpha = \gamma/2 + i\Delta$ and $\beta = (\gamma/2)\bar{n} + i\Delta'$. Equation (2.20) gives

$$\begin{aligned}\dot{\tilde{\rho}} &= \frac{\gamma}{2}(\bar{n}+1)(2\sigma_-\tilde{\rho}\sigma_+ - \sigma_+\sigma_-\tilde{\rho} - \tilde{\rho}\sigma_+\sigma_-) - i(\Delta'+\Delta)[\sigma_+\sigma_-,\tilde{\rho}]\\ &\quad + \frac{\gamma}{2}\bar{n}(2\sigma_+\tilde{\rho}\sigma_- - \sigma_-\sigma_+\tilde{\rho} - \tilde{\rho}\sigma_-\sigma_+) + i\Delta'[\sigma_-\sigma_+,\tilde{\rho}]\\ &= -i\frac{1}{2}(2\Delta'+\Delta)[\sigma_z,\tilde{\rho}] + \frac{\gamma}{2}(\bar{n}+1)(2\sigma_-\tilde{\rho}\sigma_+ - \sigma_+\sigma_-\tilde{\rho} - \tilde{\rho}\sigma_+\sigma_-)\\ &\quad + \frac{\gamma}{2}\bar{n}(2\sigma_+\tilde{\rho}\sigma_- - \sigma_-\sigma_+\tilde{\rho} - \tilde{\rho}\sigma_-\sigma_+),\end{aligned} \tag{2.24}$$

where we have used

$$\sigma_+\sigma_- = |2\rangle\langle 1|1\rangle\langle 2| = |2\rangle\langle 2| = \tfrac{1}{2}(1+\sigma_z), \tag{2.25a}$$

$$\sigma_-\sigma_+ = |1\rangle\langle 2|2\rangle\langle 1| = |1\rangle\langle 1| = \tfrac{1}{2}(1-\sigma_z). \tag{2.25b}$$

Finally, transforming back to the Schrödinger picture using (1.72), we obtain the *master equation for a radiatively damped two-level atom*:

$$\begin{aligned}\dot{\rho} = &-i\tfrac{1}{2}\omega_A'[\sigma_z,\rho] + \frac{\gamma}{2}(\bar{n}+1)(2\sigma_-\rho\sigma_+ - \sigma_+\sigma_-\rho - \rho\sigma_+\sigma_-)\\ &+ \frac{\gamma}{2}\bar{n}(2\sigma_+\rho\sigma_- - \sigma_-\sigma_+\rho - \rho\sigma_-\sigma_+),\end{aligned} \tag{2.26}$$

with

$$\omega_A' \equiv \omega_A + 2\Delta' + \Delta. \tag{2.27}$$

The symmetric grouping of terms we have adopted identifies a transition rate from $|2\rangle \to |1\rangle$, described by the term proportional to $(\gamma/2)(\bar{n}+1)$, and a transition rate from $|1\rangle \to |2\rangle$, described by the term proportional to $(\gamma/2)\bar{n}$. The former contains a rate for spontaneous transitions, independent of $\bar{n}$, and a rate for stimulated transitions induced by thermal photons, proportional to $\bar{n}$; the latter gives a rate for absorptive transitions which take thermal photons from the equilibrium electromagnetic field. We will have more to say about this point later. Notice that the Lamb shift given by $\omega_A' - \omega_A$ includes a temperature-dependent contribution $2\Delta'$ which did not appear for the harmonic oscillator. Its appearance here is a consequence of the commutator $[\sigma_-,\sigma_+] = -\sigma_z$, in place of the corresponding $[a,a^\dagger] = 1$ for the harmonic oscillator. From (2.22), (2.23), and (1.52)

$$\begin{aligned}2\Delta'+\Delta &= \sum_\lambda P\int d^3k\, \frac{g(\boldsymbol{k})|\kappa(\boldsymbol{k},\lambda)|^2}{\omega_A - kc}[1 + 2\bar{n}(kc,T)]\\ &= \sum_\lambda P\int d^3k\, \frac{g(\boldsymbol{k})|\kappa(\boldsymbol{k},T)|^2}{\omega_A - kc}\coth\left(\frac{\hbar kc}{2k_BT}\right),\end{aligned} \tag{2.28}$$

where k_B is Boltzmann's constant. The temperature independent term in the square bracket gives the normal *Lamb shift*, while the term proportional to $2\bar{n}$ gives the frequency shift induced via the ac Stark effect by the thermal reservoir field. We will discuss the ac Stark effect later in this chapter. It is only quite recently that attention has been paid to this temperature-dependent frequency shift, following the work of Gallagher and Cook [2.8]. A thorough discussion for real atoms is given by Farley and Wing [2.9]. Beautiful experiments by Hollberg and Hall using highly stabilized lasers have measured the temperature-dependent shift in Rydberg atoms [2.10].

Note 2.2 Recall from Sect. 1.4.2 that the rotating-wave approximation does not give the correct nonrelativistic result for the Lamb shift [2.11]. Actually, $(\omega_A - kc)^{-1}$ should read $(\omega_A - kc)^{-1} + (\omega_A + kc)^{-1}$ in (2.28) (Exercise 2.2).

2.2.2 The Einstein A Coefficient

If we have a correct description of spontaneous emission we must expect the damping constant γ appearing in (2.26) to give us the correct result for the Einstein A coefficient. We can check this by performing the integration over wavevectors and the polarization summation in (2.21).

Adopting spherical coordinates in $\boldsymbol{k}$-space, the density of states for each polarization state λ is given by [2.12]

$$g(\boldsymbol{k})d^3k = \frac{\omega^2 V}{8\pi^3 c^3} d\omega \sin\theta d\theta d\phi. \tag{2.29}$$

Substituting from (2.29) and (2.16) into (2.21),

$$\begin{aligned}\gamma &= 2\pi \sum_{\lambda} \int_0^{\infty} d\omega \int_0^{\pi} \sin\theta d\theta \int_0^{2\pi} d\phi \, \frac{\omega^2 V}{8\pi^3 c^3} \frac{\omega}{2\hbar\epsilon_0 V} (\hat{e}_{k,\lambda} \cdot \boldsymbol{d}_{12})^2 \delta(\omega - \omega_A) \\ &= \frac{\omega_A^3}{8\pi^2 \epsilon_0 \hbar c^3} \sum_{\lambda} \int_0^{\pi} \sin\theta d\theta \int_0^{2\pi} d\phi \, (\hat{e}_{k,\lambda} \cdot \boldsymbol{d}_{12})^2. \end{aligned} \tag{2.30}$$

Now, for each $\boldsymbol{k}$ we can choose polarization states λ_1 and λ_2 so that the first polarization state gives $\hat{e}_{k,\lambda_1} \cdot \boldsymbol{d}_{12} = 0$. This is achieved with the geometry illustrated in Fig. 2.2. Then, for the second polarization state, we find

$$(\hat{e}_{k,\lambda_2} \cdot \boldsymbol{d}_{12})^2 = d_{12}^2 (1 - \cos^2\alpha) = d_{12}^2 \left[1 - (\hat{d}_{12} \cdot \hat{k})^2\right], \tag{2.31}$$

where $\hat{d}_{12}$ and $\hat{k}$ are unit vectors in the directions of $\boldsymbol{d}_{12}$ and $\boldsymbol{k}$, respectively. The angular integrals are now easily performed if we choose the k_z-axis to correspond to the $\hat{d}_{12}$ direction. We have

$$\begin{aligned}\int_0^{\pi} \sin\theta d\theta \int_0^{2\pi} d\phi \, (\hat{e}_{k,\lambda} \cdot \boldsymbol{d}_{12})^2 &= d_{12}^2 \int_0^{2\pi} d\phi \int_0^{\pi} d\theta \sin\theta (1 - \cos^2\theta) \\ &= \frac{8\pi}{3} d_{12}^2. \end{aligned} \tag{2.32}$$

From (2.30) and (2.32)

$$\gamma = \frac{1}{4\pi\epsilon_0} \frac{4\omega_A^3 d_{12}^2}{3\hbar c^3}. \tag{2.33}$$

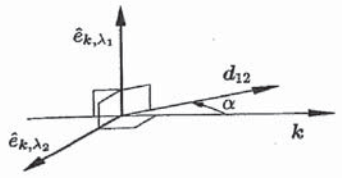

Fig. 2.2 Polarization states used in the evaluation of (2.30).

This is the correct result for the *Einstein A coefficient*, as obtained from the Wigner-Weisskopf theory of natural linewidth [2.13, 2.14].

Exercise 2.2 After replacing $(\omega_A - kc)^{-1}$ by $(\omega_A - kc)^{-1} + (\omega_A + kc)^{-1}$ in (2.23), show that this equation gives the formula for the *temperature-dependent shift* derived in Ref. [2.9]:

$$2\Delta' = \frac{1}{4\pi\epsilon_0} \frac{4d_{12}^2}{3\hbar\pi c^3} P \int_0^{\infty} d\omega \, \omega^3 \left(\frac{1}{\omega_A - \omega} + \frac{1}{\omega_A + \omega}\right) \frac{1}{e^{\hbar\omega/k_B T} - 1}. \tag{2.34}$$

The corresponding formula for the *Lamb shift* is

$$\Delta = \frac{1}{4\pi\epsilon_0} \frac{2d_{12}^2}{3\hbar\pi c^3} P \int_0^{\infty} d\omega \, \omega^3 \left(\frac{1}{\omega_A - \omega} + \frac{1}{\omega_A + \omega}\right). \tag{2.35}$$

2.2.3 Matrix Element Equations, Correlation Functions, and Spontaneous Emission Spectrum

We mentioned earlier that $\langle\sigma_z\rangle$, $\langle\sigma_-\rangle$, and $\langle\sigma_+\rangle$ are simply related to the matrix elements of ρ. We can derive equations of motion for these expectation values from (2.26) as we did for the harmonic oscillator, or, alternatively, we can simply take the matrix elements of (2.26) directly. Following the second approach, we use (2.12) to find

$$\begin{aligned}\dot{\rho}_{22} =& -i\tfrac{1}{2}\omega_A \langle 2|(\sigma_z\rho - \rho\sigma_z)|2\rangle \\ &+ \frac{\gamma}{2}(\bar{n}+1)\langle 2|(2\sigma_-\rho\sigma_+ - \sigma_+\sigma_-\rho - \rho\sigma_+\sigma_-)|2\rangle \\ &+ \frac{\gamma}{2}\bar{n}\langle 2|(2\sigma_+\rho\sigma_- - \sigma_-\sigma_+\rho - \rho\sigma_-\sigma_+)|2\rangle \\ =& -\gamma(\bar{n}+1)\rho_{22} + \gamma\bar{n}\rho_{11}, \end{aligned} \tag{2.36a}$$

and, similarly:

$$\dot{\rho}_{11} = -\gamma\bar{n}\rho_{11} + \gamma(\bar{n}+1)\rho_{22}, \tag{2.36b}$$

$$\dot{\rho}_{21} = -\left[\frac{\gamma}{2}(2\bar{n}+1) + i\omega_A\right]\rho_{21}, \tag{2.36c}$$

$$\dot{\rho}_{12} = -\left[\frac{\gamma}{2}(2\bar{n}+1) - i\omega_A\right]\rho_{12}. \tag{2.36d}$$

We have dropped the distinction between ω_A and ω_A'. Equations (2.36a) and (2.36b) clearly illustrate our interpretation of the two terms – proportional to $(\gamma/2)(\bar{n}+1)$ and $(\gamma/2)\bar{n}$ – in the master equation; the former describes $|2\rangle \rightarrow |1\rangle$ transitions at a rate $\gamma(\bar{n}+1)$, and the latter describes $|1\rangle \rightarrow |2\rangle$ transitions at a rate $\gamma\bar{n}$. Of course, probability leaves and enters the two

states in such a way that the total probability is preserved $-\dot{\rho}_{11}+\dot{\rho}_{22}=0$. Equations (2.36a) and (2.36b) are in fact just the rate equations of Einstein A and B theory.

Exercise 2.3 Show that in the steady state the balance between upwards and downwards transitions leads to a thermal equilibrium distribution between the states $|1\rangle$ and $|2\rangle$.

Using the relations $\langle\sigma_z\rangle=\rho_{22}-\rho_{11}$, $\langle\sigma_-\rangle=\rho_{21}$, $\langle\sigma_+\rangle=\rho_{12}$, and $\rho_{11}+\rho_{22}=1$, the matrix element equations can be written in the alternative form:

$$\langle\dot{\sigma}_z\rangle=-\gamma\big[\langle\sigma_z\rangle(2\bar{n}+1)+1\big], \tag{2.37a}$$

$$\langle\dot{\sigma}_-\rangle=-\Big[\frac{\gamma}{2}(2\bar{n}+1)+i\omega_A\Big]\langle\sigma_-\rangle, \tag{2.37b}$$

$$\langle\dot{\sigma}_+\rangle=-\Big[\frac{\gamma}{2}(2\bar{n}+1)-i\omega_A\Big]\langle\sigma_+\rangle. \tag{2.37c}$$

These provide us with a simple illustration of the use of the quantum regression theorem (Sect. 1.5). At optical frequencies and normal laboratory temperatures $\bar{n}$ is negligible, and for simplicity we drop it here. Then, using (2.25a), we may write the mean-value equations in vector form:

$$\langle\dot{\boldsymbol{s}}\rangle=\boldsymbol{M}\langle\boldsymbol{s}\rangle, \tag{2.38}$$

with

$$\boldsymbol{s}\equiv\begin{pmatrix}\sigma_-\\ \sigma_+\\ \sigma_+\sigma_-\end{pmatrix}, \tag{2.39}$$

$$\boldsymbol{M}\equiv\operatorname{diag}\Big[-\Big(\frac{\gamma}{2}+i\omega_A\Big),-\Big(\frac{\gamma}{2}-i\omega_A\Big),-\gamma\Big]. \tag{2.40}$$

For $\tau\geq 0$, equations for nine correlation functions are obtained from (1.107):

$$\frac{d}{d\tau}\langle\sigma_-(t)\boldsymbol{s}(t+\tau)\rangle=\boldsymbol{M}\langle\sigma_-(t)\boldsymbol{s}(t+\tau)\rangle, \tag{2.41a}$$

$$\frac{d}{d\tau}\langle\sigma_+(t)\boldsymbol{s}(t+\tau)\rangle=\boldsymbol{M}\langle\sigma_+(t)\boldsymbol{s}(t+\tau)\rangle, \tag{2.41b}$$

$$\frac{d}{d\tau}\langle\sigma_+(t)\sigma_-(t)\boldsymbol{s}(t+\tau)\rangle=\boldsymbol{M}\langle\sigma_+(t)\sigma_-(t)\boldsymbol{s}(t+\tau)\rangle. \tag{2.41c}$$

Equations for a further nine correlation functions with reverse time order are obtained from (1.108); alternatively, this second set of correlation functions can be derived from the first, using

$$\langle\hat{\boldsymbol{A}}(t+\tau)\hat{A}_\nu(t)\rangle=\langle\hat{A}_\nu^\dagger(t)\hat{\boldsymbol{A}}^\dagger(t+\tau)\rangle^*. \tag{2.42}$$

Equation (1.109) defines a further twenty-seven correlation functions.

Let us consider an atom prepared initially in its excited state. For this initial condition $\langle\sigma_-\rangle=\langle\sigma_+\rangle=0$, $\langle\sigma_+\sigma_-\rangle=\rho_{22}=1$, and the solution to (2.38) is

$$\langle\boldsymbol{s}\rangle=\begin{pmatrix}0\\ 0\\ e^{-\gamma t}\end{pmatrix}. \tag{2.43}$$

Initial conditions for (2.41a)–(2.41c) are then, respectively,

$$\langle\sigma_-(t)\boldsymbol{s}(t)\rangle=\begin{pmatrix}0\\ 1-e^{-\gamma t}\\ 0\end{pmatrix}, \tag{2.44a}$$

$$\langle\sigma_+(t)\boldsymbol{s}(t)\rangle=\begin{pmatrix}e^{-\gamma t}\\ 0\\ 0\end{pmatrix}, \tag{2.44b}$$

$$\langle\sigma_+(t)\sigma_-(t)\boldsymbol{s}(t)\rangle=\begin{pmatrix}0\\ 0\\ e^{-\gamma t}\end{pmatrix}, \tag{2.44c}$$

where we have used (2.25), together with the following:

$$\sigma_+^2=|2\rangle\langle1|2\rangle\langle1|=0, \tag{2.45a}$$

$$\sigma_-^2=|1\rangle\langle2|1\rangle\langle2|=0, \tag{2.45b}$$

$$\sigma_+\sigma_-\sigma_+=|2\rangle\langle1|1\rangle\langle2|2\rangle\langle1|=|2\rangle\langle1|=\sigma_+, \tag{2.45c}$$

$$\sigma_-\sigma_+\sigma_-=|1\rangle\langle2|2\rangle\langle1|1\rangle\langle2|=|1\rangle\langle2|=\sigma_-. \tag{2.45d}$$

The nonzero correlation functions obtained from (2.41) with initial conditions (2.44) are ($\tau\geq 0$)

$$\langle\sigma_-(t)\sigma_+(t+\tau)\rangle=e^{i\omega_A\tau}e^{-(\gamma/2)\tau}\big(1-e^{-\gamma t}\big), \tag{2.46}$$

$$\langle\sigma_+(t)\sigma_-(t+\tau)\rangle=e^{-i\omega_A\tau}e^{-(\gamma/2)\tau}e^{-\gamma t}, \tag{2.47}$$

$$\langle\sigma_+(t)\sigma_-(t)\sigma_+(t+\tau)\sigma_-(t+\tau)\rangle=e^{-\gamma\tau}e^{-\gamma t}. \tag{2.48}$$

Equation (2.47) provides the result for the *spontaneous emission spectrum*. For an ideal detector, the probability of detecting a photon of frequency ω during the interval $t=0$ to $t=T$ is given by [2.15]

$$P(\omega)\propto\int_0^T dt\int_0^T dt'\,e^{-i\omega(t-t')}\langle\sigma_+(t)\sigma_-(t')\rangle. \tag{2.49}$$

We will see how the field at the detector is related to the atomic operators σ_- and σ_+ shortly (Sect. 2.3.1); clearly, such a relationship is needed to write (2.49). Using (2.47) and

$$\langle\sigma_+(t+\tau)\sigma_-(t)\rangle=\langle\sigma_+(t)\sigma_-(t+\tau)\rangle^*, \tag{2.50}$$

we find, for all t and t',

$$\langle \sigma_+(t)\sigma_-(t')\rangle = e^{i\omega_A(t-t')}e^{-(\gamma/2)(t+t')}. \tag{2.51}$$

Then,

$$\begin{aligned} P(\omega) &\propto \int_0^T dt\, e^{-[(\gamma/2)+i(\omega-\omega_A)]t} \int_0^T dt'\, e^{-[(\gamma/2)-i(\omega-\omega_A)]t'} \\ &\propto \frac{1-e^{-(\gamma/2)T}e^{-i(\omega-\omega_A)T}}{\gamma/2+i(\omega-\omega_A)} \frac{1-e^{-(\gamma/2)T}e^{i(\omega-\omega_A)T}}{\gamma/2-i(\omega-\omega_A)}. \end{aligned} \tag{2.52}$$

For long times, $T >> 1/\gamma$, this gives the Lorentzian lineshape

$$P(\omega) \propto \frac{1}{(\gamma/2)^2+(\omega-\omega_A)^2}. \tag{2.53}$$

2.2.4 Phase Destroying Processes

The interaction with the many mode electromagnetic field that gives rise to spontaneous emission causes both energy loss from the atom and damping of the atomic polarization. Polarization damping is described by the loss terms proportional to $(\gamma/2)(2\bar{n}+1)$ in (2.36c) and (2.36d). This damping results from a randomization of the phases of the atomic wavefunctions by thermal and vacuum fluctuations in the electromagnetic field, causing the overlap of the upper and lower state wavefunctions to decay in time. It is often necessary to account for additional dephasing interactions; these might arise from elastic collisions in an atomic vapor, or elastic phonon scattering in a solid. What terms must we add to the master equation (2.26) to describe such processes?

A phenomenological model describing atomic dephasing can be obtained by adding two further reservoir interactions to the Hamiltonian (2.15). We add

$$H_{\text{dephase}} \equiv H_{R_1} + H_{R_2} + H_{SR_1} + H_{SR_2}, \tag{2.54}$$

with

$$H_{R_1} + H_{R_2} \equiv \sum_j \hbar\omega_{1j}\, r_{1j}^\dagger r_{1j} + \sum_j \hbar\omega_{2j}\, r_{2j}^\dagger r_{2j}, \tag{2.55a}$$

$$H_{SR_1} + H_{SR_2} \equiv \sum_{j,k} \hbar\kappa_{1jk}\, r_{1j}^\dagger r_{1k}\, \sigma_-\sigma_+ + \sum_{j,k} \hbar\kappa_{2jk}\, r_{2j}^\dagger r_{2k}\, \sigma_+\sigma_-. \tag{2.55b}$$

The complete reservoir seen by the atom is now composed of three subsystems: $R = R_{12} \oplus R_1 \oplus R_2$, where R_{12} is the reservoir defined by (2.15b). These reservoir subsystems are assumed to be statistically independent, with the density operator R_0 given by the product of three thermal equilibrium

operators in the form of (1.38). The interactions H_{SR_1} and H_{SR_2} describe the scattering of quanta from the atom while it is in states $|1\rangle$ and $|2\rangle$, respectively; they sum over virtual processes that scatter quanta with energies $\hbar\omega_{1k}$ and $\hbar\omega_{2k}$ into quanta with energies $\hbar\omega_{1j}$ and $\hbar\omega_{2j}$ while leaving the state of the atom unchanged.

The terms that are added to the master equation by these new reservoir interactions follow in a rather straightforward manner from the general form (1.34) for the master equation in the Born approximation. In addition to the reservoir operators $\tilde{\Gamma}_1(t)$ and $\tilde{\Gamma}_2(t)$ that are defined by the interaction with R_{12} [Eqs. (2.18)], we must introduce operators $\tilde{\Gamma}_3(t)$ and $\tilde{\Gamma}_4(t)$ to account for the interactions with R_1 and R_2. First, however, we have to take care of a problem, one which was not met in deriving master equations for the damped harmonic oscillator and the radiatively damped atom. Equation (1.34) was obtained using the assumption (1.28) that all reservoir operators coupling to the system S have zero mean in the state R_0. This is not true for the reservoir operators coupling to $\sigma_-\sigma_+$ and $\sigma_+\sigma_-$ in (2.55b); terms with $j = k$ in the summation over reservoir modes have nonzero averages proportional to mean thermal occupation numbers. To overcome this difficulty the interaction between S and the mean reservoir "field" can be included in H_S rather than H_{SR}. With the use of (2.25), in place of (2.55a) and (2.55b) we may write

$$H_S \equiv \tfrac{1}{2}\hbar(\omega_A + \delta_p)\sigma_z, \tag{2.56}$$

and

$$\begin{aligned} &H_{SR_1} + H_{SR_2} \\ &\equiv \sum_{j,k} \hbar\kappa_{1jk}(r_{1j}^\dagger r_{1k} - \delta_{jk}\bar{n}_{1j})\sigma_-\sigma_+ + \sum_{j,k} \hbar\kappa_{2jk}(r_{2j}^\dagger r_{2k} - \delta_{jk}\bar{n}_{2j})\sigma_+\sigma_-, \end{aligned} \tag{2.57}$$

with the frequency shift δ_p given by

$$\begin{aligned} \delta_p &= \sum_j (\kappa_{2jj}\bar{n}_{2j} - \kappa_{1jj}\bar{n}_{1j}) \\ &= \int_0^\infty d\omega \big[g_2(\omega)\kappa_2(\omega,\omega) - g_1(\omega)\kappa_1(\omega,\omega)\big]\bar{n}(\omega,T). \end{aligned} \tag{2.58}$$

$\bar{n}_{1j} \equiv \bar{n}(\omega_{1j},T)$ and $\bar{n}_{2j} \equiv \bar{n}(\omega_{2j},T)$ are mean occupation numbers for reservoir modes with frequencies ω_{1j} and ω_{2j}, respectively, and in (2.58) the summation over reservoir modes has been converted to an integration by introducing the densities of states $g_1(\omega)$ and $g_2(\omega)$. The sum of (2.56) and (2.57) gives the same Hamiltonian as the sum of (2.55a) and (2.55b); but now the reservoir operators that appear in H_{SR_1} and H_{SR_2} have zero mean.

We may now proceed directly from (1.34). After transforming to the interaction picture, the interaction Hamiltonian (2.57) is written in the form (1.33) with

$$\tilde{s}_3(t) = \sigma_-\sigma_+, \tag{2.59a}$$
$$\tilde{s}_4(t) = \sigma_+\sigma_-, \tag{2.59b}$$

and

$$\tilde{\Gamma}_3(t) = \sum_{j,k} \kappa_{1jk} \left(r_{1j}^\dagger r_{1k}\, e^{i(\omega_{1j}-\omega_{1k})t} - \delta_{jk}\bar{n}_{1j} \right), \tag{2.60a}$$

$$\tilde{\Gamma}_4(t) = \sum_{j,k} \kappa_{2jk} \left(r_{2j}^\dagger r_{2k}\, e^{i(\omega_{2j}-\omega_{2k})t} - \delta_{jk}\bar{n}_{2j} \right). \tag{2.60b}$$

These are to be substituted – together with $\tilde{s}_1(t)$, $\tilde{s}_2(t)$, $\tilde{\Gamma}_1(t)$, and $\tilde{\Gamma}_2(t)$ from (2.18) and (2.19) – into (1.34). Since the reservoir subsystems are statistically independent and all reservoir operators have zero mean, all of the cross terms involving correlation functions for products of operators from different reservoir subsystems will vanish. Thus, the spontaneous emission terms arising from the interaction with $\tilde{\Gamma}_1$ and $\tilde{\Gamma}_2$ are obtained exactly as in Sect. 2.2.1. The additional terms from the interaction with $\tilde{\Gamma}_3$ and $\tilde{\Gamma}_4$ take the form

$$\begin{aligned}\left(\dot{\tilde{\rho}}\right)_{\text{dephase}} = &-\int_0^t dt' [\sigma_-\sigma_+\sigma_-\sigma_+\tilde{\rho}(t') - \sigma_-\sigma_+\tilde{\rho}(t')\sigma_-\sigma_+]\langle\tilde{\Gamma}_3(t)\tilde{\Gamma}_3(t')\rangle_{R_1} \\ &+[\tilde{\rho}(t')\sigma_-\sigma_+\sigma_-\sigma_+ - \sigma_-\sigma_+\tilde{\rho}(t')\sigma_-\sigma_+]\langle\tilde{\Gamma}_3(t')\tilde{\Gamma}_3(t)\rangle_{R_1} \\ &+[\sigma_+\sigma_-\sigma_+\sigma_-\tilde{\rho}(t') - \sigma_+\sigma_-\tilde{\rho}(t')\sigma_+\sigma_-]\langle\tilde{\Gamma}_4(t)\tilde{\Gamma}_4(t')\rangle_{R_2} \\ &+[\tilde{\rho}(t')\sigma_+\sigma_-\sigma_+\sigma_- - \sigma_+\sigma_-\tilde{\rho}(t')\sigma_+\sigma_-]\langle\tilde{\Gamma}_4(t')\tilde{\Gamma}_4(t)\rangle_{R_2}.\end{aligned} \tag{2.61}$$

We will evaluate the first of the reservoir correlation functions appearing in (2.61); the others follow in a similar form. From (2.59a),

$$\begin{aligned}&\langle\tilde{\Gamma}_3(t)\tilde{\Gamma}_3(t')\rangle_{R_1} \\ &= \mathrm{tr}\Big[R_{10}\sum_{j,k}\sum_{j',k'}\kappa_{1jk}\,\kappa_{1j'k'}\left(r_{1j}^\dagger r_{1k}e^{i(\omega_{1j}-\omega_{1k})t} - \delta_{jk}\bar{n}_{1j}\right) \\ &\quad\times\left(r_{1j'}^\dagger r_{1k'}e^{i(\omega_{1j'}-\omega_{1k'})t'} - \delta_{j'k'}\bar{n}_{1j'}\right)\Big] \\ &= \mathrm{tr}\Big[R_{10}\Big(\sum_{j,k}\sum_{j',k'}\kappa_{1jk}\,\kappa_{1j'k'}\,r_{1j}^\dagger r_{1k}\,r_{1j'}^\dagger r_{1k'}\,e^{i(\omega_{1j}-\omega_{1k})t}e^{i(\omega_{1j'}-\omega_{1k'})t'} \\ &\quad-\sum_j\sum_{j',k'}\kappa_{1jj}\,\kappa_{1j'k'}\,\bar{n}_{1j}\,r_{1j'}^\dagger r_{1k'}\,e^{i(\omega_{1j'}-\omega_{1k'})t'} \\ &\quad-\sum_{j,k}\sum_{j'}\kappa_{1jk}\,\kappa_{1j'j'}\,r_{1j}^\dagger r_{1k}\,\bar{n}_{1j'}\,e^{i(\omega_{1j}-\omega_{1k})t}\Big)\Big] \\ &\quad+\sum_j\sum_{j'}\kappa_{1jj}\,\kappa_{1j'j'}\,\bar{n}_{1j}\,\bar{n}_{1j'},\end{aligned}$$

where R_{10} is the thermal equilibrium density operator [Eq. (1.38)] for the reservoir subsystem R_1. The nonvanishing contributions to the trace are now obtained as follows: the first double sum contributes for $j = k \neq j' = k'$, for $j = k' \neq k = j'$, and for $j = k = j' = k'$; the second double sum contributes for $j' = k'$; and the third double sum for $j = k$. The correlation function becomes

$$\begin{aligned}&\langle\tilde{\Gamma}_3(t)\tilde{\Gamma}_3(t')\rangle_{R_1} \\ &= \sum_{\substack{j,j'\\ j\neq j'}}\kappa_{1jj}\,\kappa_{1j'j'}\,\bar{n}_{1j}\,\bar{n}_{1j'} + \sum_{\substack{j,j'\\ j\neq j'}}\kappa_{1jj'}\,\kappa_{1j'j}\,\bar{n}_{1j}(\bar{n}_{1j'}+1)e^{i(\omega_{1j}-\omega_{1j'})(t-t')} \\ &\quad+\sum_j\kappa_{1jj}^2\overline{n_{1j}^2} - 2\sum_{j,j'}\kappa_{1jj}\,\kappa_{1j'j'}\,\bar{n}_{1j}\,\bar{n}_{1j'} + \sum_{j,j'}\kappa_{1jj}\,\kappa_{1j'j'}\,\bar{n}_{1j}\,\bar{n}_{1j'},\end{aligned}$$

where the first three terms come from the first double sum, and the fourth term comes from the second and third double sums. Noting that $\overline{n_{1j}^2} = \bar{n}_{1j}^2 + \bar{n}_{1j}(\bar{n}_{1j}+1)$, we see that the sums for $j \neq j'$ are completed for all j and j' by the third term in this expression; setting $\kappa_{1jj'}\,\kappa_{1j'j} = |\kappa_{1jj'}|^2$ – required for (2.55b) to be Hermitian – we arrive at the result

$$\langle\tilde{\Gamma}_3(t)\tilde{\Gamma}_3(t')\rangle_{R_1} = \sum_{j,j'}|\kappa_{1jj'}|^2\bar{n}_{1j}(\bar{n}_{1j'}+1)e^{i(\omega_{1j}-\omega_{1j'})(t-t')}. \tag{2.62a}$$

Similar expressions follow for the other reservoir correlation functions:

$$\langle\tilde{\Gamma}_4(t)\tilde{\Gamma}_4(t')\rangle_{R_2} = \sum_{j,j'}|\kappa_{2jj'}|^2\bar{n}_{2j}(\bar{n}_{2j'}+1)e^{i(\omega_{2j}-\omega_{2j'})(t-t')}, \tag{2.62b}$$

and

$$\langle\tilde{\Gamma}_3(t')\tilde{\Gamma}_3(t)\rangle_{R_1} = \left(\langle\tilde{\Gamma}_3(t)\tilde{\Gamma}_3(t')\rangle_{R_1}\right)^*, \tag{2.62c}$$
$$\langle\tilde{\Gamma}_4(t')\tilde{\Gamma}_4(t)\rangle_{R_2} = \left(\langle\tilde{\Gamma}_4(t)\tilde{\Gamma}_4(t')\rangle_{R_2}\right)^*. \tag{2.62d}$$

If reservoir correlation times are very short compared to the timescale for the system dynamics, the time integral in (2.61) can be treated in the same fashion as in Sect. 1.4.1. After simplifying the operator products using (2.25), (2.61) then gives

$$\left(\dot{\tilde{\rho}}\right)_{\text{dephase}} = -i\tfrac{1}{2}\Delta_p[\sigma_z,\tilde{\rho}] + \frac{\gamma_p}{2}(\sigma_z\tilde{\rho}\sigma_z - \tilde{\rho}), \tag{2.63}$$

with

$$\gamma_p \equiv \pi \int_0^\infty d\omega \left[g_2(\omega)^2 |\kappa_2(\omega,\omega)|^2 + g_1(\omega)|\kappa_1(\omega,\omega)|^2 \right] \times \bar{n}(\omega,T)\left[\bar{n}(\omega,T)+1\right], \tag{2.64}$$

$$\Delta_p \equiv P \int_0^\infty d\omega \int_0^\infty d\omega' \, \frac{g_2(\omega)g_2(\omega')|\kappa_2(\omega,\omega')|^2 - g_1(\omega)g_1(\omega')|\kappa_1(\omega,\omega')|^2}{\omega-\omega'} \times \bar{n}(\omega,T). \tag{2.65}$$

We add (2.63) to the terms describing radiative damping given by (2.24), and transform back to the Schrödinger picture using (1.72) and (2.56) to obtain the *master equation for a radiatively damped two-level atom with nonradiative dephasing*:

$$\dot{\rho} = -i\tfrac{1}{2}\omega_A'[\sigma_z,\rho] + \frac{\gamma}{2}(\bar{n}+1)(2\sigma_-\rho\sigma_+ - \sigma_+\sigma_-\rho - \rho\sigma_+\sigma_-) + \frac{\gamma}{2}\bar{n}(2\sigma_+\rho\sigma_- - \sigma_-\sigma_+\rho - \rho\sigma_-\sigma_+) + \frac{\gamma_p}{2}(\sigma_z\rho\sigma_z - \rho), \tag{2.66}$$

where the shifted atomic frequency is now

$$\omega_A' \equiv \omega_A + 2\Delta' + \Delta + \delta_p + \Delta_p, \tag{2.67}$$

with $2\Delta' + \Delta$, δ_p, and Δ_p given by (2.28), (2.58), and (2.65).

2.3 Resonance Fluorescence

The theory of resonance fluorescence provides a good illustration of the methods we have learned so far, and a simple situation in which to introduce some of the subtleties that arise in the treatment of damping for interacting atoms and fields. We are concerned here with a two-level atom irradiated by a strong monochromatic laser beam tuned to the atomic transition. Photons may be absorbed from this beam and emitted to the many modes of the vacuum electromagnetic field as fluorescent scattering. This scattering process is mediated by the reservoir interaction (2.15c) underlying our treatment of spontaneous emission.

The phenomenon of fluorescence has fascinated physicists for over a century [2.16, 2.17]. A simple classical picture can be given in terms of the Lorentz oscillator model which underlies the classical theory of dispersion [2.18–2.20]. In this picture, an harmonic electron oscillator is set into forced oscillation by the incident light and reradiates as a dipole source according to the laws of classical electrodynamics. Of course, in the absence of damping the amplitude of a resonantly forced oscillator grows without bound; to avoid this divergence some account of atomic damping must be given. In the classical theory this is achieved with the introduction of a velocity-dependent force derived from radiation reaction. The damping constant introduced in

this way ensures that the energy appearing in the reradiated field is matched by energy loss from the oscillator. This classical theory does pretty well at weak excitation. In particular, the relationship between the fluorescence spectrum and the spectrum of the excitation is correctly obtained; single-frequency excitation produces a forced response of the electron oscillator and a reradiated field with the same frequency. A hastily drawn conclusion for a two-level atom might expect the fluorescence spectrum to show the natural linewidth [Eq. (2.53)]. This would follow if the atomic dynamics proceeded by independent absorption and spontaneous emission events. However, this is an incorrect view of the scattering process. A perturbative treatment of the quantum-mechanical problem is adequate to show that at weak intensities the classical result is correct [2.21]. We must view the scattering as an essentially coherent process, passing energy from the incident beam to the scattered field without lingering en route in the excited state [2.22].

Of course, a two-level atom is not an harmonic oscillator, and the classical theory fails at sufficiently high laser intensities – in fact, it fails even at weak intensities if we look more carefully at the statistics of the scattered photons. As we will see, a two-level atom responds nonlinearly to increasing intensity; also, while an harmonic oscillator can be excited ever higher up its ladder of Fock states, a two-level atom can only store a single quantum of energy. From a quantum treatment we will find the following: With increasing incident intensity, the fluorescence spectrum picks up an incoherent component having the natural linewidth. This incoherent spectrum splits into a three-peaked structure and eventually accounts for nearly all of the scattered intensity. This behavior was first predicted by Mollow [2.23] and has been observed in a number of experiments [2.24–2.26]. The incoherent spectral component arises from quantum fluctuations around the nonequilibrium steady state established by the balance between excitation and emission processes. These quantum fluctuations are inherent in the probabilistic character of quantum dynamics, and are not introduced by any external stochastic agent.

Quantum mechanics makes its mark even at weak laser intensities if we ask the right question. We will find that there is zero probability of detecting two scattered photons emitted at the same time, independent of the incident intensity. This photon "antibunching" is a consequence of the fact that the atom can store just a single quantum of energy, and, after emitting this quantum, cannot produce a second until it is reexcited. It is the inverse of the photon "bunching" associated with the famous Hanbury-Brown-Twiss effect (Sect. 1.5.3) – there the probability for detecting two simultaneous photons is twice that expected for random photon arrivals [2.27]. Photon antibunching cannot be treated using a classical statistical description for the scattered field, and has therefore received special attention as a phenomenon requiring the quantized electromagnetic field [2.28–2.30]. The earliest reference to the vanishing probability for simultaneous photon detection in resonance fluorescence is contained in the work of Mollow [2.31]. Carmichael and Walls [2.32]

calculated the second-order correlation function for the scattered light, explicitly demonstrating antibunching in contrast to the bunching of Hanbury-Brown and Twiss. Shortly thereafter photon antibunching was observed by Kimble et al. [2.33] in the fluorescence from a dilute sodium atomic beam.

We will obtain the fluorescence spectrum and a description of photon antibunching using the master equation methods we have developed. This is not the only approach to these problems and an extensive literature is available on this subject. A good review with complete references is given by Cresser et al. [2.34].

2.3.1 The Scattered Field

The incident laser mode is in a highly excited state that is essentially unaffected by its interaction with the single atom. We can treat this field as a classical driving force. Then the Hamiltonian for the resonantly driven two-level atom interacting with the many modes of the electromagnetic field separates into system and reservoir terms, as in (1.16), with

$$H_S \equiv \tfrac{1}{2}\hbar\omega_A\sigma_z - dE\left(e^{-i\omega_A t}\sigma_+ + e^{i\omega_A t}\sigma_-\right), \tag{2.68a}$$

$$H_R \equiv \sum_{k,\lambda}\hbar\omega_k r^\dagger_{k,\lambda}r_{k,\lambda}, \tag{2.68b}$$

$$H_{SR} \equiv \sum_{k,\lambda}\hbar\left(\kappa^*_{k,\lambda}r^\dagger_{k,\lambda}\sigma_- + \kappa_{k,\lambda}r_{k,\lambda}\sigma_+\right); \tag{2.68c}$$

both interactions are written in the dipole and rotating-wave approximations. The laser field at the site of the atom is

$$\boldsymbol{E}(t) \equiv \hat{e}2E\cos(\omega_A t + \phi), \tag{2.69}$$

where $\hat{e}$ is a unit polarization vector, E is a real amplitude, and the phase ϕ is chosen so that $d \equiv \hat{e}\cdot\boldsymbol{d}_{12}e^{i\phi}$ is also real.

The master equation approach focuses on the dynamics of the atom. We are ultimately interested, however, in the properties of the fluorescence. The scattered field is given in terms of the reservoir operators – in the Heisenberg picture

$$\hat{\boldsymbol{E}}(\boldsymbol{r},t) = \hat{\boldsymbol{E}}^{(+)}(\boldsymbol{r},t) + \hat{\boldsymbol{E}}^{(-)}(\boldsymbol{r},t), \tag{2.70a}$$

with

$$\hat{\boldsymbol{E}}^{(+)}(\boldsymbol{r},t) = i\sum_{k,\lambda}\sqrt{\frac{\hbar\omega_k}{2\epsilon_0 V}}\,\hat{e}_{k,\lambda}r_{k,\lambda}(t)e^{i\boldsymbol{k}\cdot\boldsymbol{r}}, \tag{2.70b}$$

$$\hat{\boldsymbol{E}}^{(-)}(\boldsymbol{r},t) = \hat{\boldsymbol{E}}^{(+)}(\boldsymbol{r},t)^\dagger. \tag{2.70c}$$

We will need the correlation functions

$$G^{(1)}(t,t+\tau) \equiv \langle\hat{E}^{(-)}(t)\hat{E}^{(+)}(t+\tau)\rangle, \tag{2.71}$$

and

$$G^{(2)}(t,t+\tau) \equiv \langle\hat{E}^{(-)}(t)\hat{E}^{(-)}(t+\tau)\hat{E}^{(+)}(t+\tau)\hat{E}^{(+)}(t)\rangle, \tag{2.72}$$

where the field operators are evaluated at the position of an idealized point-like detector. Since we trace over the reservoir variables in deriving the master equation for S, our first task is to relate the scattered field to atomic source operators, so that (2.71) and (2.72) can be expressed in terms of operators of the system S.

We begin with the Heisenberg equations of motion for the electromagnetic field modes:

$$\dot{r}_{k,\lambda} = -i\omega_k r_{k,\lambda} - i\kappa^*_{k,\lambda}\sigma_-. \tag{2.73}$$

Writing

$$r_{k,\lambda} = \tilde{r}_{k,\lambda}e^{-i\omega_k t}, \tag{2.74a}$$

$$\sigma_- = \tilde{\sigma}_- e^{-i\omega_A t}, \tag{2.74b}$$

and integrating (2.73) formally, gives

$$\tilde{r}_{k,\lambda}(t) = r_{k,\lambda}(0) - i\kappa^*_{k,\lambda}\int_0^t dt'\,\tilde{\sigma}_-(t')e^{i(\omega_k-\omega_A)t'}. \tag{2.75}$$

The separation of the rapidly oscillating term in (2.74b) is motivated by the solution to the Heisenberg equations for the free atom [Eqs. (2.19)]. Now, substituting $r_{k,\lambda}(t)$ into (2.70a), and introducing the explicit form of the coupling constant from (2.16), the field operator becomes

$$\hat{\boldsymbol{E}}^{(+)}(\boldsymbol{r},t) = \hat{\boldsymbol{E}}^{(+)}_f(\boldsymbol{r},t) + \hat{\boldsymbol{E}}^{(+)}_s(\boldsymbol{r},t), \tag{2.76}$$

with

$$\hat{\boldsymbol{E}}^{(+)}_f(\boldsymbol{r},t) = i\sum_{k,\lambda}\sqrt{\frac{\hbar\omega_k}{2\epsilon_0 V}}\,\hat{e}_{k,\lambda}r_{k,\lambda}(0)e^{-i(\omega_k t - \boldsymbol{k}\cdot\boldsymbol{r})}, \tag{2.77}$$

and

$$\hat{\boldsymbol{E}}^{(+)}_s(\boldsymbol{r},t) = i\frac{1}{2\epsilon_0 V}e^{-i\omega_A t}\sum_{k,\lambda}\omega_k\hat{e}_{k,\lambda}(\hat{e}_{k,\lambda}\cdot\boldsymbol{d}_{12})e^{i\boldsymbol{k}\cdot(\boldsymbol{r}-\boldsymbol{r}_A)} \times\int_0^t dt'\,\tilde{\sigma}_-(t')e^{i(\omega_k-\omega_A)(t'-t)}. \tag{2.78}$$

Here $\hat{\boldsymbol{E}}^{(+)}_f(\boldsymbol{r},t)$ describes the free evolution of the electromagnetic field, in the absence of the atomic scatterer; $\hat{\boldsymbol{E}}^{(+)}_s(\boldsymbol{r},t)$ is the source field radiated by the atom. It remains to perform the summation and integration in (2.78).

The summation over $\boldsymbol{k}$ is performed by introducing the density of states (2.29) and converting the sum into an integration:

$$\hat{\boldsymbol{E}}_s^{(+)}(\boldsymbol{r},t) = i\frac{1}{16\pi^3\epsilon_0 c^3}e^{-i\omega_A t}\sum_\lambda \int_0^\infty d\omega \int_0^\pi \sin\theta\, d\theta \int_0^{2\pi} d\phi \times \omega^3 \hat{e}_{k,\lambda}(\hat{e}_{k,\lambda}\cdot\boldsymbol{d}_{12})e^{i(\omega r/c)\cos\theta}\int_0^t dt'\,\tilde{\sigma}_-(t')e^{i(\omega-\omega_A)(t'-t)}; \tag{2.79}$$

we have chosen a geometry with the origin in $\boldsymbol{r}$-space at the site of the atom and the k_z-axis in the direction of $\boldsymbol{r}$. One polarization state may be chosen perpendicular to both $\boldsymbol{k}$ and $\boldsymbol{d}_{12}$, as in Fig. 2.2, and for the second we can write

$$\hat{e}_{k,\lambda_2}(\hat{e}_{k,\lambda_2}\cdot\boldsymbol{d}_{12}) = -\hat{e}_{k,\lambda_2}d_{12}\sin\alpha = -(\boldsymbol{d}_{12}\times\hat{k})\times\hat{k}, \tag{2.80}$$

where $\hat{k}$ is a unit vector in the direction of $\boldsymbol{k}$. Setting

$$\hat{k} = \hat{r}\cos\theta + \hat{k}_x\sin\theta\cos\phi + \hat{k}_y\sin\theta\sin\phi, \tag{2.81}$$

where $\hat{k}_x$, $\hat{k}_y$, and $\hat{r}\equiv\boldsymbol{r}/r$ are unit vectors along the Cartesian axes in $\boldsymbol{k}$-space, the angular integrals are then readily evaluated to give

$$\hat{\boldsymbol{E}}_s^{(+)}(\boldsymbol{r},t) = \frac{1}{8\pi^2\epsilon_0 c^2 r}(\boldsymbol{d}_{12}\times\hat{r})\times\hat{r}\int_0^\infty d\omega\,\omega^2\Bigg[e^{-i\omega_A(t+r/c)} \times\int_0^t dt'\,\tilde{\sigma}_-(t')e^{i(\omega-\omega_A)(t'-t-r/c)} - e^{-i\omega_A(t-r/c)} \times\int_0^t dt'\,\tilde{\sigma}_-(t')e^{i(\omega-\omega_A)(t'-t+r/c)}\Bigg]. \tag{2.82}$$

Now, since the transformation (2.74b) removes the rapid oscillation at the atomic resonance frequency, $\tilde{\sigma}_-$ is expected to vary slowly in comparison with the optical period – on a time scale characterized by $\gamma^{-1}\sim 10^{-8}$s (for optical frequencies), compared with $\omega_A^{-1}\sim 10^{-15}$s. Thus, for frequencies outside the range $-100\gamma\le\omega-\omega_A\le 100\gamma$, say, the time integrals in (2.82) average to zero. This means that over the important range of the frequency integral $\omega^2\approx\omega_A^2+2(\omega-\omega_A)\omega_A$ varies by less than 0.01% from $\omega^2=\omega_A^2$. We therefore replace ω^2 by ω_A^2 and extend the frequency integral to $-\infty$. We then find

$$\begin{aligned}\hat{\boldsymbol{E}}_s^{(+)}(\boldsymbol{r},t) &= \frac{\omega_A^2}{4\pi\epsilon_0 c^2 r}(\boldsymbol{d}_{12}\times\hat{r})\times\hat{r}\left[e^{-i\omega_A(t+r/c)}\int_0^t dt'\,\tilde{\sigma}_-(t')\delta(t'-t-r/c)\right.\\ &\quad\left. - e^{-i\omega_A(t-r/c)}\int_0^t dt'\,\tilde{\sigma}_-(t')\delta(t'-t+r/c)\right]\\ &= -\frac{\omega_A^2}{4\pi\epsilon_0 c^2 r}(\boldsymbol{d}_{12}\times\hat{r})\times\hat{r}\,\sigma_-(t-r/c).\end{aligned} \tag{2.83}$$

This is precisely the familiar result for classical dipole radiation with the dipole moment *operator* $\boldsymbol{d}_{12}\sigma_-$ in place of the classical dipole moment.

Since thermal effects are negligible at optical frequencies ($\hbar\omega_A >> k_BT$), we will take the reservoir state to correspond to the vacuum electromagnetic field – the thermal equilibrium state at $T=0$. Then, the free field (2.77) makes no contribution to normal-ordered correlation functions such as (2.71) and (2.72); thus, from (2.83) we may now write

$$G^{(1)}(t+r/c,t+r/c+\tau) = f(\boldsymbol{r})\langle\sigma_+(t)\sigma_-(t+\tau)\rangle, \tag{2.84}$$

and

$$G^{(2)}(t+r/c,t+r/c+\tau) = f(\boldsymbol{r})^2\langle\sigma_+(t)\sigma_+(t+\tau)\sigma_-(t+\tau)\sigma_-(t)\rangle. \tag{2.85}$$

$f(\boldsymbol{r})$ is the geometrical factor

$$f(\boldsymbol{r}) \equiv \left(\frac{\omega_A^2 d_{12}}{4\pi\epsilon_0 c^2}\right)^2\frac{\sin^2\theta}{r^2}, \tag{2.86}$$

where θ is the angle between $\boldsymbol{d}_{12}$ and $\boldsymbol{r}$. (Recall that $\boldsymbol{r}$ measures positions with respect to an origin at the location of the atom.)

2.3.2 Master Equation for a Two-Level Atom Driven by a Classical Field

In deriving the master equation for resonance fluorescence we may go directly to (1.34), with s_1, s_2, Γ_1, and Γ_2 identified as in (2.17). We meet only one minor difference from our treatment of spontaneous emission in proceeding from this equation to the final result: The reservoir operators in the interaction picture are again given by (2.18); but the system operators $\tilde{s}_1$ and $\tilde{s}_2$ are now given by

$$\tilde{s}_1(t) = \sigma_-(t) \equiv \exp\left[(i/\hbar)\int_0^t dt' H_S(t')\right]\sigma_-\exp\left[-(i/\hbar)\int_0^t dt' H_S(t')\right], \tag{2.87a}$$

$$\tilde{s}_2(t) = \sigma_+(t) \equiv \exp\left[(i/\hbar)\int_0^t dt' H_S(t')\right]\sigma_+\exp\left[-(i/\hbar)\int_0^t dt' H_S(t')\right], \tag{2.87b}$$

where H_S includes the interaction with the laser. What effect does this interaction have on the atomic damping? It will turn out, in fact, that any changes in the treatment of the damping are negligible under normal conditions. However, let us spend some time discussing this question anyway so that we have an idea of the approximation involved. The same approximation is made, often without mention, in laser theory and in cavity QED.

Equations (2.87) are just the formal solutions to the Heisenberg equations of motion for the atom-field interaction described by Hamiltonian (2.68a). These equations are given by

$$\begin{aligned}\dot{\sigma}_- &= \frac{1}{i\hbar}[\sigma_-, H_S] \\ &= -i\tfrac{1}{2}\omega_A[\sigma_-, \sigma_z] + i\left(\frac{d}{\hbar}E\right)e^{-i\omega_A t}[\sigma_-, \sigma_+] \\ &= -i\omega_A\sigma_- - i\left(\frac{d}{\hbar}E\right)e^{-i\omega_A t}\sigma_z, \end{aligned} \tag{2.88a}$$

and, similarly,

$$\dot{\sigma}_+ = i\omega_A\sigma_+ + i\left(\frac{d}{\hbar}E\right)e^{i\omega_A t}\sigma_z, \tag{2.88b}$$

$$\dot{\sigma}_z = 2i\left(\frac{d}{\hbar}E\right)e^{-i\omega_A t}\sigma_+ - 2i\left(\frac{d}{\hbar}E\right)e^{i\omega_A t}\sigma_-. \tag{2.88c}$$

Defining

$$\tilde{\sigma}_x \equiv \sigma_+ e^{-i\omega_A t} + \sigma_- e^{i\omega_A t}, \tag{2.89a}$$

$$i\tilde{\sigma}_y \equiv \sigma_+ e^{-i\omega_A t} - \sigma_- e^{i\omega_A t}, \tag{2.89b}$$

(2.88a)–(2.88c) become

$$\dot{\tilde{\sigma}}_x = 0, \tag{2.90a}$$

$$\dot{\tilde{\sigma}}_y = \Omega\sigma_z, \tag{2.90b}$$

$$\dot{\sigma}_z = -\Omega\tilde{\sigma}_y, \tag{2.90c}$$

where

$$\Omega \equiv 2\left(\frac{d}{\hbar}E\right). \tag{2.91}$$

In particular, from (2.90b) and (2.90c),

$$\ddot{\sigma}_z = -\Omega^2\sigma_z. \tag{2.92}$$

Then, for an atom initially in its lower state [$\langle\tilde{\sigma}_y(0)\rangle = 0$, $\langle\sigma_z(0)\rangle = -1$],

$$\langle\sigma_z(t)\rangle = -\cos\Omega t. \tag{2.93}$$

Ω is the *Rabi frequency* [2.30]; the frequency at which the atom periodically cycles between its lower and upper states, following absorption from the laser field with stimulated emission, then again absorption, and so on.

The general solution to (2.90) is

$$\tilde{s}_1(t) = \sigma_-(t) = e^{-i\omega_A t}\left[\sigma_- + \tfrac{1}{2}(1-\cos\Omega t)(\sigma_+ - \sigma_-) - \tfrac{1}{2}i(\sin\Omega t)\sigma_z\right], \tag{2.94a}$$

$$\tilde{s}_2(t) = \sigma_+(t) = e^{i\omega_A t}\left[\sigma_+ - \tfrac{1}{2}(1-\cos\Omega t)(\sigma_+ - \sigma_-) + \tfrac{1}{2}i(\sin\Omega t)\sigma_z\right], \tag{2.94b}$$

where $\sigma_+ = \sigma_+(0)$, $\sigma_- = \sigma_-(0)$, and $\sigma_z = \sigma_z(0)$ denote operators in the Schrödinger picture. Our derivation of the master equation for spontaneous emission proceeded from (1.34) with $\tilde{s}_1(t)$ and $\tilde{s}_2(t)$ given by the expression (2.94) taken in the limit $\Omega \to 0$. The interaction with the laser field has introduce terms modulated at the Rabi frequency. Now, there is no difficulty with substituting the full solutions (2.94) into (1.34) and continuing by performing the time integrals as before. The number of terms to be considered is increased nine fold, however, and we do not want to churn through all of this algebra if it is not really necessary. A quick review of our calculation for the damped harmonic oscillator will show that the oscillatory terms in $\tilde{s}_1(t)$ and $\tilde{s}_2(t)$ only specify the frequencies at which the system interacts with the reservoir; they determine the frequencies at which we evaluate the reservoir coupling constant and density of states. The final result following from (2.94) will then be an equation that contains three terms, each proportional to one of the three damping constants $\gamma(\omega_A)$, $\gamma(\omega_A+\Omega)$, and $\gamma(\omega_A-\Omega)$, where $\gamma(\omega_A)$ is given by (2.21), and $\gamma(\omega_A+\Omega)$ and $\gamma(\omega_A-\Omega)$ are similarly defined with the reservoir coupling constant and density of states evaluated at shifted frequencies. At optical frequencies and reasonable laser intensities $\omega_A \sim 10^{15}$, and $\Omega < 10^{10}$ (this corresponds to 100 times the saturation intensity for sodium). Then, from (2.33),

$$\gamma(\omega_A \pm \Omega) = \gamma(\omega_A)(1 \pm \Omega/\omega_A)^3 \approx \gamma(\omega_A)(1 \pm 3\Omega/\omega_A). \tag{2.95}$$

Thus, $\gamma(\omega_A \pm \Omega)$ differs from $\gamma = \gamma(\omega_A)$ by less than 0.01%. We therefore neglect Ω compared with ω_A. This is best done in (2.94) rather than at the end of a lot of tedious algebra. Setting Ω to zero in (2.94) is equivalent to deriving the master equation in an interaction picture with H_S replaced by the free Hamiltonian $\frac{1}{2}\hbar\omega_A\sigma_z$. Then the damping terms in the master equation for resonance fluorescence are the same as those derived for spontaneous emission. Neglecting thermal effects ($\bar{n} = 0$), the *master equation for resonance fluorescence* is then

$$\begin{aligned}\dot{\rho} = &-i\tfrac{1}{2}\omega_A[\sigma_z, \rho] + i(\Omega/2)\left[e^{-i\omega_A t}\sigma_+ + e^{i\omega_A t}\sigma_-, \rho\right] \\ &+ \frac{\gamma}{2}(2\sigma_-\rho\sigma_+ - \sigma_+\sigma_-\rho - \rho\sigma_+\sigma_-). \end{aligned} \tag{2.96}$$

In fact, a similar approximation was made, without mention, in our derivation of the scattered field, where we assume σ_- oscillates at the frequency ω_A [Eq. (2.74b)]. Further discussion of these issues, with specific consideration of their relevance in the Scully-Lamb theory of the laser, is given by Carmichael and Walls [2.36, 2.37].

Note 2.3 Recent work by Lewenstein et al. [2.38, 2.39] describes a situation in which the near equality of the damping constants $\gamma(\omega_A)$, $\gamma(\omega_A+\Omega)$, and $\gamma(\omega_A-\Omega)$ does not hold. This happens for an atom inside an optical cavity when the interaction between the atom and the vacuum modes it sees through the cavity mirrors significantly perturbs the free-space interaction between the atom and the vacuum field. Under these conditions the vacuum modes which are filtered by the cavity have a Lorentzian density of states that can vary considerably at the frequencies ω_A, $\omega_A+\Omega$, and $\omega_A-\Omega$. The consequent changes in the three damping constants alter the widths of the peaks in the fluorescence spectrum. Lewenstein et al. formulate their treatment of this effect in terms of non-Markovian equations for the damped atom. This is not necessary, however, if the Lorentzian feature in the density of states is narrower than (or similar in width to) the Rabi frequency, but is still much broader than the linewidths $\gamma(\omega_A)$, $\gamma(\omega_A+\Omega)$, and $\gamma(\omega_A-\Omega)$ (computed with the altered density of states). The method of Carmichael and Walls [2.36, 2.37] is appropriate for these conditions and leads to a Markovian master equation; but one in which the variation of the density of reservoir modes at the three different atomic frequencies is taken into account.

2.3.3 Optical Bloch Equations and Dressed States

Using the quantum regression theorem, our derivation of the correlation functions appearing in (2.84) and (2.85) will follow directly from the equations of motion for the operator expectation values $\langle\sigma_-\rangle$, $\langle\sigma_+\rangle$, and $\langle\sigma_z\rangle$. Using the master equation (2.96), these are given by

$$\langle\dot\sigma_-\rangle = -i\omega_A\langle\sigma_-\rangle - i(\Omega/2)e^{-i\omega_A t}\langle\sigma_z\rangle - \frac{\gamma}{2}\langle\sigma_-\rangle, \tag{2.97a}$$

$$\langle\dot\sigma_+\rangle = i\omega_A\langle\sigma_+\rangle + i(\Omega/2)e^{i\omega_A t}\langle\sigma_z\rangle - \frac{\gamma}{2}\langle\sigma_+\rangle, \tag{2.97b}$$

$$\langle\dot\sigma_z\rangle = i\Omega e^{-i\omega_A t}\langle\sigma_+\rangle - i\Omega e^{i\omega_A t}\langle\sigma_-\rangle - \gamma\big(\langle\sigma_z\rangle+1\big). \tag{2.97c}$$

These are the *optical Bloch equations* with radiative damping, so called for their relationship to the equations of a spin-$\frac{1}{2}$ particle in a magnetic field [2.40]. They combine the terms describing the atom-field interaction given by (2.88) with the spontaneous decay terms in (2.37).

Note 2.4 When the phase destroying term $(\gamma_p/2)(\sigma_z\rho\sigma_z-\rho)$ in (2.66) is included in the master equation, (2.97a) and (2.97b) have γ replaced by $\gamma+2\gamma_p$. The energy and phase decay times $1/\gamma$ and $2/(\gamma+2\gamma_p)$, respectively, are often denoted by T_1 and T_2 in correspondence with the traditional terminology for magnetic systems.

If we neglect the effects of spontaneous decay, which is valid for short times, the optical Bloch equations are equivalent to the classical equations

for a magnetic moment $\boldsymbol{m}$ in a rotating magnetic field $\boldsymbol{B}$. With $\langle\sigma_x\rangle$ and $\langle\sigma_y\rangle$ defined as in (2.9), we can write

$$\dot{\boldsymbol{m}} = \boldsymbol{B}\times\boldsymbol{m}, \tag{2.98}$$

where

$$\boldsymbol{m} \equiv \langle\sigma_x\rangle\hat{x} + \langle\sigma_y\rangle\hat{y} + \langle\sigma_z\rangle\hat{z}, \tag{2.99}$$

and

$$\boldsymbol{B} \equiv -(\Omega\cos\omega_A t)\hat{x} - (\Omega\sin\omega_A t)\hat{y} + \omega_A\hat{z}; \tag{2.100}$$

$\hat{x}$, $\hat{y}$, and $\hat{z}$ are orthogonal unit vectors. A strong intuition for the dynamics in resonance fluorescence can be drawn from this analogy. From (2.98) it follows that

$$\begin{aligned}\frac{d}{dt}(\boldsymbol{m}\cdot\boldsymbol{m}) &= (\boldsymbol{B}\times\boldsymbol{m})\cdot\boldsymbol{m} + \boldsymbol{m}\cdot(\boldsymbol{B}\times\boldsymbol{m})\\ &= 0,\end{aligned} \tag{2.101}$$

since $\boldsymbol{m}$ and $\boldsymbol{B}\times\boldsymbol{m}$ are perpendicular vectors. Thus, $\boldsymbol{m}$ is a vector of constant length. In particular, for pure states, with

$$\rho = |\psi\rangle\langle\psi| = \big(c_1|1\rangle + c_2|2\rangle\big)\big(\langle 1|c_1^* + \langle 2|c_2^*\big), \tag{2.102}$$

we have

$$\langle\sigma_-\rangle = \rho_{21} = c_1^*c_2, \tag{2.103a}$$

$$\langle\sigma_+\rangle = \rho_{12} = c_1c_2^*, \tag{2.103b}$$

$$\langle\sigma_z\rangle = \rho_{22} - \rho_{11} = |c_2|^2 - |c_1|^2, \tag{2.103c}$$

and

$$\begin{aligned}\boldsymbol{m}\cdot\boldsymbol{m} &= \langle\sigma_x\rangle^2 + \langle\sigma_y\rangle^2 + \langle\sigma_z\rangle^2\\ &= 4\langle\sigma_-\rangle\langle\sigma_+\rangle + \langle\sigma_z\rangle^2\\ &= \big(|c_1|^2 + |c_2|^2\big)^2.\end{aligned} \tag{2.104}$$

Thus, for a pure state $\boldsymbol{m}\cdot\boldsymbol{m} = 1$, and (2.101) expresses the requirement that probability be conserved. Here the state of the two-level atom can be represented by a point on the surface of the unit sphere (the *Bloch sphere*) as illustrated in Fig. 2.3(b). Dynamics on the Bloch sphere give a simple interpretation for the solutions (2.93) and (2.94). We define a rotating frame of reference which follows the rotating magnetic field, writing

$$\tilde{\boldsymbol{m}} \equiv \boldsymbol{R}_z(\omega_A t)\boldsymbol{m} = \begin{pmatrix}\cos\omega_A t & \sin\omega_A t & 0\\ -\sin\omega_A t & \cos\omega_A t & 0\\ 0 & 0 & 1\end{pmatrix}\boldsymbol{m}, \tag{2.105}$$

where $\boldsymbol{R}_z$ generates rotations about the z-axis. The motion of $\tilde{\boldsymbol{m}}$ is then determined by a magnetic field frozen in the $\hat{x}$ direction:

$$\dot{\tilde{\boldsymbol{m}}} = (\tilde{\boldsymbol{B}} - \omega_A \hat{z}) \times \tilde{\boldsymbol{m}}, \tag{2.106}$$

where $\tilde{\boldsymbol{B}} \equiv \boldsymbol{R}_z(\omega_A t)\boldsymbol{B}$ and

$$\tilde{\boldsymbol{B}} - \omega_A \hat{z} = -\Omega \hat{x}. \tag{2.107}$$

The modulation at the Rabi frequency shown by (2.93) and (2.94) simply corresponds to the precession of $\tilde{\boldsymbol{m}}$ about the static magnetic field $\tilde{\boldsymbol{B}} - \omega_A \hat{z}$ [Fig. 2.3(c)].

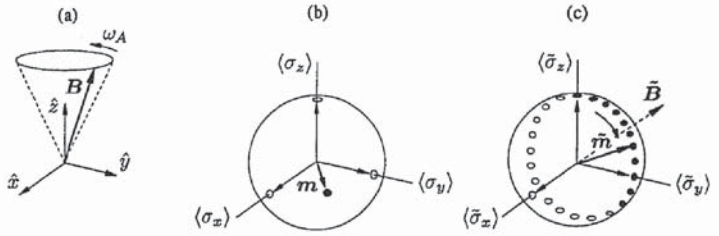

Fig. 2.3 Representation of atomic dynamics on the Bloch sphere: (a) the rotating magnetic field (2.100), (b) the atomic state represented as a point on the Bloch sphere, (c) precession of the atomic state in the rotating frame (2.105).

This simple view of the dynamics no longer provides the complete picture when the dissipative terms are reintroduced. Then (2.97a)–(2.97c) give

$$\begin{aligned}\frac{d}{dt}(\boldsymbol{m}\cdot\boldsymbol{m}) &= 2\big(\langle\sigma_x\rangle\langle\dot{\sigma}_x\rangle + \langle\sigma_y\rangle\langle\dot{\sigma}_y\rangle + \langle\sigma_z\rangle\langle\dot{\sigma}_z\rangle\big)\\ &= -\gamma\Big[\langle\sigma_x\rangle^2 + \langle\sigma_y\rangle^2 + 2\langle\sigma_z\rangle\big(\langle\sigma_z\rangle + 1\big)\Big]\\ &= -\gamma(\boldsymbol{m}\cdot\boldsymbol{m} - 1) - \gamma\big(\langle\sigma_z\rangle + 1\big)^2.\end{aligned} \tag{2.108}$$

Now the length of $\boldsymbol{m}$ is not conserved. This is not inconsistent with (2.104). Probability is still conserved, but the atomic state has become a mixed state, rather than a pure state; therefore (2.104) no longer gives a valid interpretation for $\boldsymbol{m}\cdot\boldsymbol{m}$. Dynamics cannot be formulated on the Bloch sphere. In fact, evolution proceeds to a steady state, with

$$\boldsymbol{m}\cdot\boldsymbol{m} = 1 - \big(\langle\sigma_z\rangle + 1\big)^2 = 1 - 4\rho_{22}^2, \tag{2.109}$$

which has the state $\boldsymbol{m}$ *within* the unit sphere. Since $\boldsymbol{m}\cdot\boldsymbol{m}$ must be greater than zero, it follows that $\rho_{22} \leq \frac{1}{2}$ in the steady state. Thus, interaction with the laser field can at best give equal probability for finding the atom in its upper and lower states – it cannot produce population inversion. Of course, a higher probability of excitation is possible during transients, which for an

intense laser (large enough Ω) closely resemble the precession on the Bloch sphere which we have just described.

Exercise 2.4 Solve the optical Bloch equations (2.97). Show that, for an atom initially in its lower state,

$$\begin{aligned}e^{\pm i\omega_A t}\langle\sigma_\mp(t)\rangle = \pm i\frac{1}{\sqrt{2}}\frac{Y}{1+Y^2}\left[1 - e^{-(3\gamma/4)t}\left(\cosh\delta t + \frac{(3\gamma/4)}{\delta}\sinh\delta t\right)\right]\\ \pm i\sqrt{2}Y e^{-(3\gamma/4)t}\frac{(\gamma/4)}{\delta}\sinh\delta t,\end{aligned} \tag{2.110}$$

$$\langle\sigma_z(t)\rangle = -\frac{1}{1+Y^2}\left[1 + Y^2 e^{-(3\gamma/4)t}\left(\cosh\delta t + \frac{(3\gamma/4)}{\delta}\sinh\delta t\right)\right], \tag{2.111}$$

where

$$Y \equiv \frac{\sqrt{2}\Omega}{\gamma}, \tag{2.112}$$

$$\delta \equiv \sqrt{\left(\frac{\gamma}{4}\right)^2 - \Omega^2} = \frac{\gamma}{4}\sqrt{1 - 8Y^2}. \tag{2.113}$$

In the limit $\gamma << \Omega$, $\gamma t << 1$, show that these solutions reproduce the dynamics on the Bloch sphere discussed above.

A complementary view of the atomic dynamics is given by the *dressed-states formalism* whose application to the problem of resonance fluorescence has been championed by Cohen-Tannoudji and Reynaud [2.41]. In this formalism we focus on the eigenstates of H_S, from which a full picture of the dynamics without damping can be constructed in the Schrödinger picture. It is usual to develop the dressed-states formalism around the fully quantized Hamiltonian

$$H_S \equiv \tfrac{1}{2}\hbar\omega_A\sigma_z + \hbar\omega_A a^\dagger a + \hbar(\kappa a\sigma_+ + \kappa^* a^\dagger\sigma_-), \tag{2.114}$$

rather than the time-dependent (semiclassical) Hamiltonian (2.68a). Here $a^\dagger$ and a are creation and annihilation operators for the laser mode, and the free Hamiltonian $\hbar\omega_A a^\dagger a$ generates the time dependence – $a(t) = a(0)e^{-i\omega_A t}$; to make the connection with (2.68a) we must take $\hbar\kappa\langle a\rangle = -dE$.

Without the atom-field interaction the eigenvalues of H_S define the infinite ladder of degenerate energy levels illustrated in Fig. 2.4(a). States $|n\rangle|2\rangle$ and $|n+1\rangle|1\rangle$ correspond to an n-photon Fock state plus an excited atom, and an $(n+1)$-photon Fock state plus an unexcited atom, respectively; both have the energy $\big(n + \frac{1}{2}\big)\hbar\omega_A$. This degeneracy is lifted by the interaction. The size of the resulting level splitting may be found, together with the new energy eigenstates, by diagonalizing the coupled equations

$$H_S\begin{pmatrix}|n\rangle|2\rangle\\ |n+1\rangle|1\rangle\end{pmatrix} = \begin{pmatrix}\big(n+\frac{1}{2}\big)\hbar\omega_A & \sqrt{n+1}\,\hbar\kappa^*\\ \sqrt{n+1}\,\hbar\kappa & \big(n+\frac{1}{2}\big)\hbar\omega_A\end{pmatrix}\begin{pmatrix}|n\rangle|2\rangle\\ |n+1\rangle|1\rangle\end{pmatrix}. \tag{2.115}$$

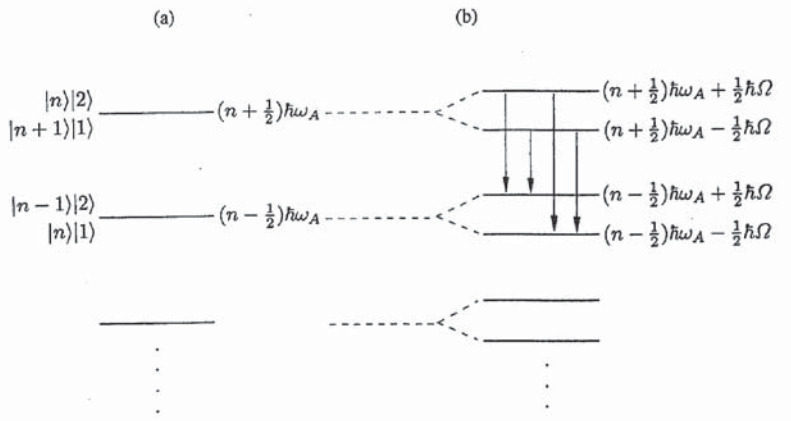

Fig. 2.4 (a) Degenerate ladder of energy levels for the uncoupled atom-field system. (b) Level splitting due to the atom-field interaction. Reading from left to right, the illustrated transitions have frequencies ω_A, $\omega_A - \Omega$, $\omega_A + \Omega$, and ω_A.

The new energy eigenvalues are

$$E_{n,\pm} = (n+\tfrac{1}{2})\hbar\omega_A \pm \sqrt{n+1}\,\hbar|\kappa|. \tag{2.116}$$

If the laser field is in a coherent state with mean photon number $\bar{n} >> 1$, we may write

$$dE = \hbar|\kappa||\langle a|| = \hbar|\kappa|\sqrt{\bar{n}},$$

and for all the populated eigenstates

$$E_{n,\pm} \approx (n+\tfrac{1}{2})\hbar\omega_A \pm \hbar\left(\frac{d_{12}}{\hbar}E\right) = (n+\tfrac{1}{2})\hbar\omega_A \pm \tfrac{1}{2}\hbar\Omega. \tag{2.117}$$

Transitions between the eigenstates of the interacting atom-field system identify the three frequencies ω_A, $\omega_A + \Omega$, and $\omega_A - \Omega$ encountered in (2.94) [Fig. 2.4(b)]. The three damping constants that arose in our treatment of the fluorescent decay process (Sect. 2.3.2) may now be associated with fluorescent transitions between the states of the coupled atom-field system – the so-called *dressed states*. If we suppress the $n\hbar\omega_A$ which distinguishes states of the Fock hierarchy, the remaining four-level structure gives the *dressed energies* $-\frac{1}{2}\hbar(\omega_A \mp \Omega)$ and $+\frac{1}{2}\hbar(\omega_A \pm \Omega)$ for the atom.

Exercise 2.5 Construct the eigenvectors corresponding to the eigenvalues (2.116) and hence find explicit expressions for the dressed states as linear combinations of the states $|n\rangle|2\rangle$ and $|n+1\rangle|1\rangle$. For large n the dressed states approximately factorize as the product of a Fock state for the field

and linear combinations of the states $|2\rangle$ and $|1\rangle$ for the atom (neglect the difference between $|n\rangle$ and $|n+1\rangle$). Locate the atomic states obtained after the factorization on the Bloch sphere.

Note 2.5 The dressed states are often referred to as the dressed states of the atom. Clearly, the states obtained by diagonalizing (2.115) should not really be referred to in this way, since these states are vectors within the Hilbert space of the atom *plus the field*. There are, nonetheless, conditions under which it is appropriate to ascribe the "dressing" to states of the atom alone – in the large n limit mentioned in Exercise 2.5. There are a number of ways to give a mathematically well-defined meaning to this limit. If we start within the Hilbert space of the atom plus quantized field mode, we must define an approximation scheme that maps all the four-level structures in Fig. (2.4b) (with $n \approx \bar{n}$) to a single four-level structure that does not distinguish between photon numbers, and in this way defines the levels of the dressed atom. Perhaps a more satisfactory approach is to begin from the semiclassical Hamiltonian (2.68a). This Hamiltonian is time dependent and does not, therefore, define a normal eigenvalue problem. But it is periodic in time. For such a Hamiltonian periodic solutions to the Schrödinger equation and their associated quasienergies play the role of energy eigenstates and eigenvalues [2.42, 2.43]. It is easy to find these periodic states and quasienergies for the Hamiltonian (2.68a): first transform to the interaction picture, diagonalize the resulting time-independent Hamiltonian, and then transform back to the Schrödinger picture. The quasienergies found in this way are the energies $-\frac{1}{2}\hbar(\omega_A \mp \Omega)$ and $+\frac{1}{2}\hbar(\omega_A \pm \Omega)$ defined above as the dressed energies of the atom.

2.3.4 The Fluorescence Spectrum

We might expect the spectrum of the fluorescent scattering to show features associated with the three transition frequencies between dressed states, ω_A, $\omega_A + \Omega$, and $\omega_A - \Omega$. Although this seems an obvious conclusion to draw from Fig. 2.4(b), there is really little basis for accepting it a priori. For weak excitation by monochromatic light, the fluorescence spectrum is shown by perturbation theory to also be monochromatic [2.21] – it does not have the linewidth of spontaneous emission. This teaches us that the scattering process is not simply a sequence of absorption and emission events; there is some coherence involved; a view of the quantum dynamics based solely on discrete transitions between atomic energy levels is not to be trusted. Moreover, consider the mean scattered field given by (2.83) and (2.110). For strong excitation this does contain components at the shifted frequencies $\omega_A \pm \Omega$. These decay, however, as transients and in the long-time limit

$$\lim_{t\to\infty}\langle \hat{\boldsymbol{E}}_s^{(+)}(\boldsymbol{r},t)\rangle = -\frac{\omega_A^2}{4\pi\epsilon_0 c^2 r}(\boldsymbol{d}_{12}\times\hat{\boldsymbol{r}})\times\hat{\boldsymbol{r}}\left(i\frac{1}{\sqrt{2}}\frac{Y}{1+Y^2}\right)e^{-i\omega_A(t-r/c)}. \tag{2.118}$$

Equation (2.118) suggests monochromatic fluorescence, in agreement with the established weak-field result. The dynamical picture is one of coherent reradiation from an induced dipole oscillator, the excitation strength entering only to saturate the oscillator amplitude.

Surely, however, this essentially classical picture is also incomplete. The quantum-mechanical dipole operator lives in a probabilistic world, and therefore we should allow our oscillator amplitude the opportunity to acquire a stochastic component. Then, in general, the fluorescence spectrum should not be calculated from the mean scattered field, but from the Fourier transform of the autocorrelation function (2.71). Using (2.84), for the long-time limit, this gives

$$S(\omega) = f(\boldsymbol{r})\frac{1}{2\pi}\int_{-\infty}^{\infty} d\tau\, e^{i\omega\tau}\langle\sigma_+(0)\sigma_-(\tau)\rangle_{\rm ss}, \tag{2.119}$$

where $\langle\sigma_+(0)\sigma_-(\tau)\rangle_{\rm ss} \equiv \lim_{t\to\infty}\langle\sigma_+(t)\sigma_-(t+\tau)\rangle$. Thus, in a rotating frame, the atomic scatterer decays to the steady state

$$\langle\tilde{\sigma}_\mp\rangle_{\rm ss} = e^{\pm i\omega_A t}\langle\sigma_\mp\rangle_{\rm ss} = \pm i\frac{1}{\sqrt{2}}\frac{Y}{1+Y^2}, \tag{2.120a}$$

$$\langle\sigma_z\rangle_{\rm ss} = -\frac{1}{1+Y^2}. \tag{2.120b}$$

However, fluctuations about this steady state can occur, described by the operators

$$\Delta\tilde{\sigma}_\mp \equiv \tilde{\sigma}_\mp - \langle\tilde{\sigma}_\mp\rangle_{\rm ss}, \tag{2.121a}$$

$$\Delta\sigma_z \equiv \sigma_z - \langle\sigma_z\rangle_{\rm ss}. \tag{2.121b}$$

These fluctuations are intrinsic to the quantum mechanics. Now the fluorescence spectrum decomposes into a coherent component, corresponding to (2.118), and an incoherent component arising from quantum fluctuations:

$$S(\omega) = S_{\rm coh}(\omega) + S_{\rm inc}(\omega), \tag{2.122}$$

with

$$\begin{aligned} S_{\rm coh}(\omega) &= f(\boldsymbol{r})\frac{1}{2\pi}\int_{-\infty}^{\infty} d\tau\, e^{i(\omega-\omega_A)\tau}\langle\tilde{\sigma}_+\rangle_{\rm ss}\langle\tilde{\sigma}_-\rangle_{\rm ss} \\ &= f(\boldsymbol{r})\frac{1}{2}\frac{Y^2}{(1+Y^2)^2}\,\delta(\omega-\omega_A), \end{aligned} \tag{2.123}$$

and

$$S_{\rm inc}(\omega) = f(\boldsymbol{r})\frac{1}{2\pi}\int_{-\infty}^{\infty} d\tau\, e^{i(\omega-\omega_A)\tau}\langle\Delta\tilde{\sigma}_+(0)\Delta\tilde{\sigma}_-(\tau)\rangle_{\rm ss}. \tag{2.124}$$

Let $I_{\rm coh}$ and $I_{\rm inc}$ denote the coherent and incoherent intensities obtained by integrating (2.123) and (2.124) over all frequencies:

$$\begin{aligned} I_{\rm coh} &= f(\boldsymbol{r})\langle\tilde{\sigma}_+\rangle_{\rm ss}\langle\tilde{\sigma}_-\rangle_{\rm ss} \\ &= f(\boldsymbol{r})\frac{1}{2}\frac{Y^2}{(1+Y^2)^2}, \end{aligned} \tag{2.125}$$

and

$$\begin{aligned} I_{\rm inc} &= f(\boldsymbol{r})\langle\Delta\tilde{\sigma}_+\Delta\tilde{\sigma}_-\rangle_{\rm ss} \\ &= f(\boldsymbol{r})\big(\langle\tilde{\sigma}_+\tilde{\sigma}_-\rangle_{\rm ss} - \langle\tilde{\sigma}_+\rangle_{\rm ss}\langle\tilde{\sigma}_-\rangle_{\rm ss}\big) \\ &= f(\boldsymbol{r})\big[\tfrac{1}{2}\big(1+\langle\sigma_z\rangle_{\rm ss}\big) - \langle\tilde{\sigma}_+\rangle_{\rm ss}\langle\tilde{\sigma}_-\rangle_{\rm ss}\big] \\ &= f(\boldsymbol{r})\frac{1}{2}\frac{Y^4}{(1+Y^2)^2}. \end{aligned} \tag{2.126}$$

We can now make a judgment about the qualitative form of the spectrum. At weak laser intensities, the ratio $I_{\rm inc}/I_{\rm coh} = Y^2 = 2\Omega^2/\gamma^2$ is very small, and coherent scattering dominates, in agreement with the results from perturbation theory. However, $I_{\rm inc}/I_{\rm coh}$ increases with the laser intensity, and the incoherent spectral component will dominate at high laser intensities. Since the relaxation, or regression, of fluctuations around the steady state must surely follow a modulated decay similar to that shown by (2.110) and (2.111), we expect this incoherent spectrum to show sidebands at $\omega_A \pm \Omega$. The general dynamical picture must then be constructed as something of a mixture, showing both elements of coherent reradiation and discrete quantum transitions.

Note 2.6 The face the quantum dynamics shows to us depends on the questions we ask, as is generally the case in quantum mechanics. Illustrating this, we might note that the radiated intensity admits an interpretation in terms of discrete quantum transitions even at weak excitation, where $I_{\rm coh}(\boldsymbol{r})$ dominates. If $I(\boldsymbol{r}) = I_{\rm coh}(\boldsymbol{r}) + I_{\rm inc}(\boldsymbol{r}) = f(\boldsymbol{r})\langle\tilde{\sigma}_+\tilde{\sigma}_-\rangle_{\rm ss}$ is the total intensity at the position $\boldsymbol{r}$, we can integrate over a sphere of radius r (centered on the atom) to obtain the radiated power:

$$\begin{aligned} P &= 2\epsilon_0 c\int_0^{2\pi} d\phi\int_0^{\pi} d\theta\sin\theta\, r^2 I(\boldsymbol{r}) \\ &= 2\epsilon_0 c\left(\frac{\omega_A^2 d_{12}}{4\pi\epsilon_0 c^2}\right)^2\left(\int_0^{2\pi} d\phi\int_0^{\pi} d\theta\sin^3\theta\right)\langle\tilde{\sigma}_+\tilde{\sigma}_-\rangle_{\rm ss} \\ &= \left(\frac{1}{4\pi\epsilon_0}\frac{4\omega_A^3 d_{12}^2}{3\hbar c^3}\right)\hbar\omega_A\,\langle 2|\rho_{\rm ss}|2\rangle \\ &= \gamma\,\hbar\omega_A\,\langle 2|\rho_{\rm ss}|2\rangle. \end{aligned} \tag{2.127}$$

The radiated power is just the product of the atomic decay rate, the photon energy carried away per emission, and the probability that the atom is in its excited state. We have an interpretation in terms of discrete spontaneous

emission events, despite the fact that the weak-field spectrum is not consistent with these dynamics.

The approach we have outlined for calculating the fluorescence spectrum is essentially the same as that followed by Mollow [2.23] in his original work. It certainly leads to a simple calculation compared to some of those that rederived Mollow's result (see Cresser et al. [2.34] for a review). We need only solve for $\langle \Delta\tilde{\sigma}_+(0)\Delta\tilde{\sigma}_-(\tau)\rangle_{ss}$ using the optical Bloch equations and the quantum regression theorem. From (2.97), (2.120), and (2.121),

$$\frac{d}{dt}\langle \Delta\tilde{\sigma}_-\rangle = -i(\Omega/2)\langle \Delta\sigma_z\rangle - \frac{\gamma}{2}\langle \Delta\tilde{\sigma}_-\rangle, \tag{2.128a}$$

$$\frac{d}{dt}\langle \Delta\tilde{\sigma}_+\rangle = i(\Omega/2)\langle \Delta\sigma_z\rangle - \frac{\gamma}{2}\langle \Delta\tilde{\sigma}_+\rangle, \tag{2.128b}$$

$$\frac{d}{dt}\langle \Delta\sigma_z\rangle = i\Omega\langle \Delta\tilde{\sigma}_+\rangle - i\Omega\langle \Delta\tilde{\sigma}_-\rangle - \gamma\langle \Delta\sigma_z\rangle, \tag{2.128c}$$

and the quantum regression theorem gives

$$\frac{d}{d\tau}\langle \Delta\tilde{\sigma}_+(0)\Delta\boldsymbol{s}(\tau)\rangle_{ss} = \boldsymbol{M}\langle \Delta\tilde{\sigma}_+(0)\Delta\boldsymbol{s}(\tau)\rangle_{ss}, \tag{2.129}$$

where

$$\Delta\boldsymbol{s} \equiv \begin{pmatrix} \Delta\tilde{\sigma}_- \\ \Delta\tilde{\sigma}_+ \\ \Delta\sigma_z \end{pmatrix}, \tag{2.130}$$

and

$$\boldsymbol{M} \equiv -\frac{\gamma}{2}\begin{pmatrix} 1 & 0 & iY/\sqrt{2} \\ 0 & 1 & -iY/\sqrt{2} \\ i\sqrt{2}Y & -i\sqrt{2}Y & 2 \end{pmatrix}. \tag{2.131}$$

The desired correlation function is the first component of the vector $\langle \Delta\tilde{\sigma}_+(0)\Delta\boldsymbol{s}(\tau)\rangle_{ss}$. The initial conditions are given by

$$\begin{aligned}\langle \Delta\tilde{\sigma}_+\Delta\boldsymbol{s}\rangle_{ss} &= \begin{pmatrix} \langle\tilde{\sigma}_+\tilde{\sigma}_-\rangle_{ss} - \langle\tilde{\sigma}_+\rangle_{ss}\langle\tilde{\sigma}_-\rangle_{ss} \\ \langle\tilde{\sigma}_+\tilde{\sigma}_+\rangle_{ss} - \langle\tilde{\sigma}_+\rangle^2_{ss} \\ \langle\tilde{\sigma}_+\sigma_z\rangle_{ss} - \langle\tilde{\sigma}_+\rangle_{ss}\langle\sigma_z\rangle_{ss} \end{pmatrix} \\ &= \begin{pmatrix} \frac{1}{2}\big(1+\langle\sigma_z\rangle_{ss}\big) - \langle\tilde{\sigma}_+\rangle_{ss}\langle\sigma_-\rangle_{ss} \\ -\langle\tilde{\sigma}_+\rangle^2_{ss} \\ -\langle\tilde{\sigma}_+\rangle_{ss}\big(1+\langle\sigma_z\rangle_{ss}\big) \end{pmatrix},\end{aligned}$$

where we have used (2.25), (2.45), and

$$\sigma_+\sigma_z = |2\rangle\langle 1|\big(|2\rangle\langle 2| - |1\rangle\langle 1|\big) = -|2\rangle\langle 1| = -\sigma_+, \tag{2.132a}$$

$$\sigma_-\sigma_z = |1\rangle\langle 2|\big(|2\rangle\langle 2| - |1\rangle\langle 1|\big) = |1\rangle\langle 2| = \sigma_-. \tag{2.132b}$$

From the steady-state averages (2.120) we obtain

$$\langle \Delta\tilde{\sigma}_+\Delta\boldsymbol{s}\rangle_{ss} = \frac{1}{2}\frac{Y^2}{(1+Y^2)^2}\begin{pmatrix} Y^2 \\ 1 \\ i\sqrt{2}Y \end{pmatrix}. \tag{2.133}$$

Equation (2.129) can be solve by finding a matrix $\boldsymbol{S}$ to diagonalize $\boldsymbol{M}$. Multiplying (2.129) on the left by $\boldsymbol{S}$,

$$\frac{d}{d\tau}\boldsymbol{S}\langle \Delta\tilde{\sigma}_+(0)\Delta\boldsymbol{s}(\tau)\rangle_{ss} = (\boldsymbol{S}\boldsymbol{M}\boldsymbol{S}^{-1})\boldsymbol{S}\langle \Delta\tilde{\sigma}_+(0)\Delta\boldsymbol{s}(\tau)\rangle_{ss}, \tag{2.134}$$

and, formally,

$$\langle \Delta\tilde{\sigma}_+(0)\Delta\boldsymbol{s}(\tau)\rangle_{ss} = \boldsymbol{S}^{-1}\exp(\boldsymbol{\lambda}\tau)\boldsymbol{S}\langle \Delta\tilde{\sigma}_+\Delta\boldsymbol{s}\rangle_{ss}, \tag{2.135}$$

where

$$\boldsymbol{\lambda} \equiv \boldsymbol{S}\boldsymbol{M}\boldsymbol{S}^{-1} = \mathrm{diag}\left(-\frac{\gamma}{2}, -\frac{3\gamma}{4}+\delta, -\frac{3\gamma}{4}-\delta\right) \tag{2.136}$$

is formed from the eigenvalues of $\boldsymbol{M}$, and the rows (columns) of $\boldsymbol{S}$ ($\boldsymbol{S}^{-1}$) are the left (right) eigenvectors of $\boldsymbol{M}$ [2.44]; δ is defined in (2.113). After some algebra we obtain the *first-order correlation function for resonance fluorescence*

$$\begin{aligned}&\langle \Delta\tilde{\sigma}_+(0)\Delta\tilde{\sigma}_-(\tau)\rangle_{ss} \\ &\quad= \frac{1}{4}\frac{Y^2}{1+Y^2}e^{-(\gamma/2)\tau} \\ &\qquad -\frac{1}{8}\frac{Y^2}{(1+Y^2)^2}\left[1-Y^2+(1-5Y^2)\frac{(\gamma/4)}{\delta}\right]e^{-[(3\gamma/4)-\delta]\tau} \\ &\qquad -\frac{1}{8}\frac{Y^2}{(1+Y^2)^2}\left[1-Y^2-(1-5Y^2)\frac{(\gamma/4)}{\delta}\right]e^{-[(3\gamma/4)+\delta]\tau}.\end{aligned} \tag{2.137}$$

Explicit expressions for the incoherent spectrum can be calculated from (2.124) and (2.137) as an exercise. In general, the spectrum is given by a sum of three Lorentzian components. It is easy to see that in the strong-field limit, $Y^2 >> 1$ ($\Omega^2 >> \gamma^2$), where incoherent scattering dominates, this calculation gives the well-known Mollow, or Stark, triplet. Figure 2.5 illustrates the dependence of the incoherent component of the fluorescence spectrum on the laser intensity.

2.3.5 Second-Order Coherence

We have identified "coherent" scattering with a monochromatic spectrum. More precisely, a monochromatic spectrum only implies first-order coherence – i.e. when $\langle \Delta\tilde{\sigma}_+(0)\Delta\tilde{\sigma}_-(\tau)\rangle_{ss}$ vanishes the first-order correlation function factorizes:

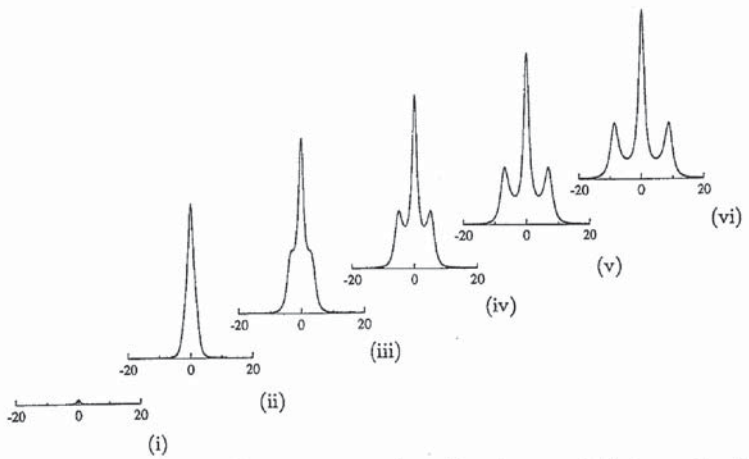

Fig. 2.5 The incoherent fluorescence spectrum. Spectra are plotted as a function of $2(\omega-\omega_A)/\gamma$ for (i) $Y=0.3$, (ii) $Y=1.5$, (iii) $Y=2.7$, (iv) $Y=3.9$, (v) $Y=5.1$, and $Y=6.3$.

$$G^{(1)}_{ss}(\tau) = f(\boldsymbol{r})\langle\sigma_+(0)\sigma_-(\tau)\rangle_{ss} = f(\boldsymbol{r})\langle\sigma_+\rangle_{ss}\langle\sigma_-\rangle_{ss}e^{-i\omega_A\tau},$$

where $G^{(1)}_{ss}(\tau) \equiv \lim_{t\to\infty} G^{(1)}(t,t+\tau)$. This guarantees nothing about higher-order correlation functions. Do they factorize in a similar fashion? Is the scattered light in the weak-field limit – where the spectrum is monochromatic – coherent to all orders, as would be the radiation from a classical dipole? It is not difficult to see that it is not. We need look no further than to the second-order correlation function; the scattered light does not have second-order coherence. The lack of second-order coherence is associated with the phenomenon of photon antibunching. It tells us that the fluorescence from a two-level atom is nonclassical, even in the weak-field limit where a model based on classical dipole radiation gives the correct spectrum.

The second-order correlation function is proportional to the probability for the detection of two photons separated by a delay time τ. It is measured in delayed photon coincidence experiments [2.45, 2.46].

Note 2.7 Actual photodetection probabilities depend on such things as the photon counting time and the collection and quantum efficiencies of the detector. In (2.127) we saw that the photon emission rate into a 4π solid angle is $\gamma\langle\sigma_+\sigma_-\rangle_{ss}$ (the radiated power is $\hbar\omega_A\gamma\langle\sigma_+\sigma_-\rangle_{ss}$). Consider a detector located at position $\boldsymbol{r}$ which accepts photons over the small solid angle $\Delta\Omega$, and has a detection efficiency η. The single-photon detection probability during a short counting interval $\Delta T << \gamma^{-1}$ is the product of the energy density $2\epsilon_0\langle\hat{E}^{(-)}\hat{E}^{(+)}\rangle_{ss}$, a factor $c/\hbar\omega_A$ which convert this into a photon flux density,

the detector area $\Delta\Omega r^2$, photon counting time ΔT, and quantum efficiency η:

$$\begin{aligned} p(1) &= \eta\Delta T(\Delta\Omega r^2)\frac{2\epsilon_0 c}{\hbar\omega_A}G^{(1)}_{ss}(0) \\ &= \eta\gamma\Delta T\frac{\Delta\Omega\sin^2\theta}{8\pi/3}\langle\sigma_+\sigma_-\rangle_{ss}. \end{aligned} \tag{2.138}$$

After integration over all solid angles this gives $p(1) = \eta\gamma\Delta T\langle\sigma_+\sigma_-\rangle_{ss} = \eta\gamma\Delta T\langle 2|\rho_{ss}|2\rangle$, in agreement with (2.127). The probability for detecting a first photon *and* a second photon after a delay τ is

$$\begin{aligned} p(2,\tau;1,0) &= \left[\eta\Delta T(\Delta\Omega r^2)\frac{2\epsilon_0 c}{\hbar\omega_A}\right]^2 G^{(2)}_{ss}(\tau) \\ &= \left[\eta\gamma\Delta T\frac{\Delta\Omega\sin^2\theta}{8\pi/3}\right]^2 \langle\sigma_+(0)\sigma_+(\tau)\sigma_-(\tau)\sigma_-(0)\rangle_{ss}. \end{aligned} \tag{2.139}$$

This result is proportional to the second-order correlation function (2.85).

In the long-time limit, second-order coherence requires the second-order correlation function to factorize in the form

$$G^{(2)}_{ss}(\tau) = f(\boldsymbol{r})^2\langle\sigma_+(0)\sigma_+(\tau)\sigma_-(\tau)\sigma_-(0)\rangle_{ss} = \left[f(\boldsymbol{r})\langle\sigma_+\rangle_{ss}\langle\sigma_-\rangle_{ss}\right]^2;$$

this factorization must hold in addition to the requirement for first-order coherence stated above. It clearly never holds for $\tau = 0$, since $\langle\sigma_+\rangle^2_{ss}$ and $\langle\sigma_-\rangle^2_{ss}$ are not zero [from (2.120a)] but $\sigma_+^2 = \sigma_-^2 = 0$. The latter simply states that a two-level atom cannot be sequentially raised or lowered twice; two photons cannot be absorbed or emitted simultaneously; the detection of one photon sets the atom in its lower state, after which a second photon cannot be detected until the atom has been reexcited. We might predict then that the probability for detecting two photons is just the probability for detecting the first photon,

$$p(1) \propto f(\boldsymbol{r})\langle\sigma_+\sigma_-\rangle_{ss} = f(\boldsymbol{r})\langle 2|\rho_{ss}|2\rangle,$$

multiplied by the probability for detecting a second photon at the time $t=\tau$, given that the atom was in its lower state at $t=0$:

$$p(2,\tau|1,0) \propto f(\boldsymbol{r})\langle(\sigma_+\sigma_-)(\tau)\rangle_{\rho(0)=|1\rangle\langle 1|} = f(\boldsymbol{r})\langle 2|\rho(\tau)|2\rangle_{\rho(0)=|1\rangle\langle 1|}.$$

We are suggesting that the second-order correlation function may be factorized as a product of photon detection probabilities, with

$$G^{(2)}_{ss}(\tau) = f(\boldsymbol{r})^2\langle 2|\rho_{ss}|2\rangle\langle 2|\rho(\tau)|2\rangle_{\rho(0)=|1\rangle\langle 1|}. \tag{2.140}$$

This is clearly zero for $\tau = 0$, and gives independent detection events for large τ, as $\rho(\tau)\to\rho_{ss}$. We will use the quantum regression theorem to prove

this result. (As with the calculation of the fluorescence spectrum, other approaches can be used to obtain this result; Kimble and Mandel, for example, derive (2.140) working entirely in the Heisenberg picture [2.47].)

First, let us consider the formal solution to the Bloch equations for time-dependent expectation values. In a rotating frame, (2.97a)–(2.97c) can be written in the vector form

$$\langle \dot{\boldsymbol{s}} \rangle = \boldsymbol{M}\langle \boldsymbol{s} \rangle + \boldsymbol{b}, \tag{2.141}$$

where

$$\boldsymbol{s} \equiv \begin{pmatrix} \tilde{\sigma}_- \\ \tilde{\sigma}_+ \\ \sigma_z \end{pmatrix}, \tag{2.142}$$

$\boldsymbol{M}$ is the 3×3 matrix given by (2.131), and

$$\boldsymbol{b} \equiv -\gamma \begin{pmatrix} 0 \\ 0 \\ 1 \end{pmatrix}. \tag{2.143}$$

Then

$$\frac{d}{dt}\big(\langle \boldsymbol{s} \rangle + \boldsymbol{M}^{-1}\boldsymbol{b}\big) = \boldsymbol{M}\big(\langle \boldsymbol{s} \rangle + \boldsymbol{M}^{-1}\boldsymbol{b}\big), \tag{2.144}$$

and

$$\langle \boldsymbol{s}(t) \rangle = -\boldsymbol{M}^{-1}\boldsymbol{b} + \exp(\boldsymbol{M}t)\big(\langle \boldsymbol{s}(0) \rangle + \boldsymbol{M}^{-1}\boldsymbol{b}\big). \tag{2.145}$$

Now

$$\begin{aligned} G^{(2)}_{\rm ss}(\tau) &= f(\boldsymbol{r})^2 \langle \sigma_+(0)\sigma_+(\tau)\sigma_-(\tau)\sigma_-(0)\rangle_{\rm ss} \\ &= f(\boldsymbol{r})^2 \tfrac{1}{2}\big[\langle \sigma_+\sigma_-\rangle_{\rm ss} + \langle \sigma_+(0)\sigma_z(\tau)\sigma_-(0)\rangle_{\rm ss}\big], \end{aligned} \tag{2.146}$$

where we have used (2.25a). We can calculate the correlation function $\langle \sigma_+(0)\sigma_z(\tau)\sigma_-(0)\rangle_{\rm ss}$ using the quantum regression theorem. It is the third component of the vector $\langle \sigma_+ \boldsymbol{s}(\tau)\sigma_-\rangle_{\rm ss}$. To find the equation of motion for this vector, the quantum regression theorem tells us to remove the angular brackets from (2.141) ($\boldsymbol{b}$ is a constant vector multiplied by the expectation of the identity operator), multiply on the left by $\sigma_+(0)$ and on the right by $\sigma_-(0)$, and replace the angular brackets; thus

$$\begin{aligned} \frac{d}{d\tau}\langle \sigma_+(0)\boldsymbol{s}(\tau)\sigma_-(0)\rangle_{\rm ss} &= \boldsymbol{M}\langle \sigma_+(0)\boldsymbol{s}(\tau)\sigma_-(0)\rangle_{\rm ss} + \langle \sigma_+\sigma_-\rangle_{\rm ss}\boldsymbol{b} \\ &= \boldsymbol{M}\big[\langle \sigma_+(0)\boldsymbol{s}(\tau)\sigma_-(0)\rangle_{\rm ss} + \langle \sigma_+\sigma_-\rangle_{\rm ss}\boldsymbol{M}^{-1}\boldsymbol{b}\big]. \end{aligned} \tag{2.147}$$

The formal solution to this equation is

$$\begin{aligned} \langle \sigma_+(0)\boldsymbol{s}(\tau)\sigma_-(0)\rangle_{ss} = &-\langle \sigma_+\sigma_-\rangle_{\rm ss}\boldsymbol{M}^{-1}\boldsymbol{b} \\ &+ \exp(\boldsymbol{M}\tau)\big[\langle \sigma_+\boldsymbol{s}\,\sigma_-\rangle_{\rm ss} + \langle \sigma_+\sigma_-\rangle_{\rm ss}\boldsymbol{M}^{-1}\boldsymbol{b}\big], \end{aligned} \tag{2.148}$$

with initial conditions

$$\begin{aligned} \langle \sigma_+\boldsymbol{s}\,\sigma_-\rangle_{\rm ss} &= \begin{pmatrix} \langle \sigma_+\tilde{\sigma}_-\sigma_-\rangle_{\rm ss} \\ \langle \sigma_+\tilde{\sigma}_+\sigma_-\rangle_{\rm ss} \\ \langle \sigma_+\sigma_z\sigma_-\rangle_{\rm ss} \end{pmatrix} \\ &= \langle \sigma_+\sigma_-\rangle_{\rm ss}\begin{pmatrix} 0 \\ 0 \\ -1 \end{pmatrix}, \end{aligned} \tag{2.149}$$

where we have used (2.45) and (2.132). Now (2.148), (2.149), and (2.145) give

$$\begin{aligned} &\langle \sigma_+(0)\boldsymbol{s}(\tau)\sigma_-(0)\rangle_{\rm ss} \\ &\quad = \langle \sigma_+\sigma_-\rangle_{\rm ss}\left\{-\boldsymbol{M}^{-1}\boldsymbol{b} + \exp(\boldsymbol{M}\tau)\left[\begin{pmatrix} 0 \\ 0 \\ -1 \end{pmatrix} + \boldsymbol{M}^{-1}\boldsymbol{b}\right]\right\} \\ &\quad = \langle \sigma_+\sigma_-\rangle_{\rm ss}\langle \boldsymbol{s}(\tau)\rangle_{\rho(0)=|1\rangle\langle 1|}. \end{aligned} \tag{2.150}$$

Here, we have noted that $\begin{pmatrix} 0 \\ 0 \\ -1 \end{pmatrix}$ is simply the initial condition $\langle \boldsymbol{s}(0)\rangle$ for an atom prepared in its lower state – i.e. with $\rho(0) = |1\rangle\langle 1|$. Substituting the third component of (2.150) into (2.146) establishes our result:

$$\begin{aligned} G^{(2)}_{\rm ss}(\tau) &= f(\boldsymbol{r})^2 \langle \sigma_+\sigma_-\rangle_{\rm ss}\tfrac{1}{2}\big(1 + \langle \sigma_z(\tau)\rangle_{\rho(0)=|1\rangle\langle 1|}\big) \\ &= f(\boldsymbol{r})^2 \langle 2|\rho_{\rm ss}|2\rangle\langle 2|\rho(\tau)|2\rangle_{\rho(0)=|1\rangle\langle 1|}. \end{aligned} \tag{2.151}$$

Note that this calculation is independent of the form of $\boldsymbol{M}$. Thus, while (2.131) only gives $\boldsymbol{M}$ for perfect resonance, (2.151) also holds for nonresonant excitation.

Note 2.8 The factorized result we have obtained in (2.151) actually follows very simply, and quite generally, from the quantum regression theorem written in the more formal form (1.102):

$$\begin{aligned} G^{(2)}_{\rm ss}(\tau) &= f(\boldsymbol{r})^2 \langle \sigma_+(0)\sigma_+(\tau)\sigma_-(\tau)\sigma_-(0)\rangle_{\rm ss} \\ &= f(\boldsymbol{r})^2 {\rm tr}\big\{e^{\mathcal{L}\tau}\big[\sigma_-(0)\rho_{\rm ss}\sigma_+(0)\big]\sigma_+(0)\sigma_-(0)\big\} \\ &= f(\boldsymbol{r})^2 {\rm tr}\big\{e^{\mathcal{L}\tau}\big[|1\rangle\langle 2|\rho_{\rm ss}|2\rangle\langle 1|\big]|2\rangle\langle 2|\big\} \\ &= f(\boldsymbol{r})^2 \langle 2|\rho_{\rm ss}|2\rangle\langle 2|e^{\mathcal{L}\tau}\big(|1\rangle\langle 1|\big)|2\rangle; \end{aligned}$$

$\langle 2|e^{\mathcal{L}\tau}\big(|1\rangle\langle 1|\big)|2\rangle$ is just a formal expression for $\langle 2|\rho(\tau)|2\rangle_{\rho(0)=|1\rangle\langle 1|}$.

Equation (2.111) provides the solution for $\langle \sigma_z(t)\rangle_{\rho(0)=|1\rangle\langle 1|}$ from which an explicit expression for $G^{(2)}_{\rm ss}(\tau)$ may be written down. We normalize $G^{(2)}_{\rm ss}(\tau)$ by

its factorized form for independent photon detection in the large-delay limit, and write the *second-order correlation function for resonance fluorescence* as

$$\begin{aligned} g_{ss}^{(2)}(\tau) &\equiv \left[\lim_{\tau\to\infty} G_{ss}^{(2)}(\tau)\right]^{-1} G_{ss}^{(2)}(\tau) \\ &= \left(\langle\sigma_+\sigma_-\rangle_{ss}\right)^{-1}\left(1+\langle\sigma_z(\tau)\rangle_{\rho(0)=|1\rangle\langle 1|}\right) \\ &= 1-e^{-(3\gamma/4)\tau}\left(\cosh\delta\tau+\frac{3\gamma/4}{\delta}\sinh\delta\tau\right). \end{aligned} \tag{2.152}$$

This expression is plotted in Fig. 2.6. For a field possessing second-order coherence $g_{ss}^{(2)}(\tau)=1$; the two photons are detected independently for all decay times; in this case a detector responds to the incident light by producing a completely random sequence of photopulses. This picture provides a reference against which the "antibunching" of photopulses is defined. The curves of Fig. 2.6 actually show two nonclassical features – features that are inadmissible in a correlation function generated by a classical stationary stochastic process. Let us look at the definitions of photon antibunching that have been given in terms of each.

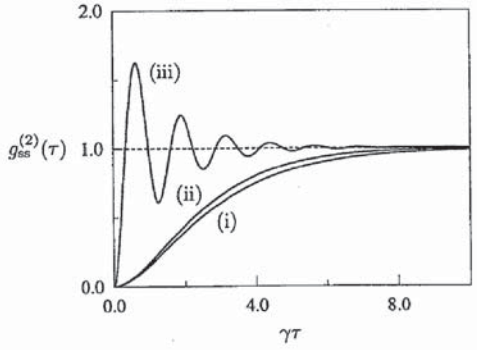

Fig. 2.6 The normalized second-order correlation function (2.152): (i) $8Y^2 = 0.01 \ll 1$ ($\delta \approx \gamma/4$); (ii) $8Y^2 = 1$ ($\delta = 0$); (iii) $8Y^2 = 400 \gg 1$ ($\delta \approx i\Omega$).

2.3.6 Photon Antibunching and Squeezing

All of the curves in Fig. 2.6 satisfy the inequality

$$g_{ss}^{(2)}(0) < 1. \tag{2.153}$$

This is the definition of photon antibunching given in Refs. [2.28–2.30, 2.32]. The sense of this definition is actually more clearly understood by considering

a closely related quantity to $g_{ss}^{(2)}(\tau)$. Imagine a photopulse sequence generated by a fast photodetector – response time much faster than $\min(\gamma^{-1}, \Omega^{-1})$ – monitoring the fluorescence. The quantity we will focus on is the probability density $w_{ss}(\tau)$ for a delay τ between successive photopulses, a quantity we refer to as the *photoelectron waiting-time distribution*. This can be calculated as the probability density that, given a photopulse at time t, there is also a photopulse at time $t+\tau$, *conditioned on the requirement that there are no photopulses in the intervening interval*; thus, the photopulse at time $t+\tau$ is the *next* photopulse in the sequence. For comparison, $\Delta T^{-1}[p(2,\tau;1,0)/p(1)] = \Delta T^{-1} p(1) g_{ss}^{(2)}(\tau)$ [Eqs. (2.138) and (2.139)] gives the probability density for a photopulse at $t+\tau$ *without any restriction on photopulses in the intervening interval*. The distribution $w_{ss}(\tau)$ must satisfy

$$\int_0^\infty d\tau\, w_{ss}(\tau) = 1, \tag{2.154}$$

since the delay between photopulses must take some value between zero and infinity; $\Delta T^{-1} p(1) g_{ss}^{(2)}(\tau)$ does not have to satisfy such a condition.

To clarify the notation we write

$$\begin{aligned} \Delta T^{-1} p(1) &= \eta\left(\frac{3}{8\pi}\int_{\substack{\text{solid}\\ \text{angle}}} d\Omega\,\sin^2\theta\right)\gamma\langle\sigma_+\sigma_-\rangle_{ss} \\ &= \eta'\gamma\langle\sigma_+\sigma_-\rangle_{ss}, \end{aligned} \tag{2.155}$$

where we have allowed for detection over an arbitrary solid angle, and $0 < \eta' \leq 1$ is the product of the collection and quantum efficiencies of the detector; $\gamma\langle\sigma_+\sigma_-\rangle_{ss}$ is the photon emission rate. The functions $w_{ss}(\tau)$ and $\left(\eta'\gamma\langle\sigma_+\sigma_-\rangle_{ss}\right) g_{ss}^{(2)}(\tau)$ approach each other for $\tau \ll \tau_{av}$, where τ_{av} is the average time between photopulses, since the probability for intervening photopulses becomes small in this limit. In particular, $w_{ss}(0) = \left(\eta'\gamma\langle\sigma_+\sigma_-\rangle_{ss}\right) g_{ss}^{(2)}(0)$. For longer time intervals, coherent scattering would give the waiting-time distribution

$$w_{ss}(\tau) = \eta'\gamma\langle\sigma_+\sigma_-\rangle_{ss}\exp\left(-\eta'\gamma\langle\sigma_+\sigma_-\rangle_{ss}\tau\right). \tag{2.156}$$

In fact, a calculation of $w_{ss}(\tau)$ for $\eta' \ll 1$ (which holds under the most readily achievable experimental conditions [2.48, 2.49]) produces the result [2.50]

$$\begin{aligned} w_{ss}(\tau) \approx \eta'\gamma\langle\sigma_+\sigma_-\rangle_{ss}\Big[&\exp\left(-\eta'\gamma\langle\sigma_+\sigma_-\rangle_{ss}\tau\right) - e^{-(3\gamma/4)\tau} \\ &\times\left(\cosh\delta\tau+\frac{3\gamma/4}{\delta}\sinh\delta\tau\right)\Big] \end{aligned} \tag{2.157}$$

for the *photoelectron waiting-time distribution of resonance fluorescence at low detection efficiency*. This expression satisfies (2.154) to lowest order in η'. It should be compared with the expression for $(\eta'\gamma\langle\sigma_+\sigma_-\rangle_{ss})g^{(2)}_{ss}(\tau)$ given by (2.152). The two expressions agree for $\tau \ll (\eta'\gamma\langle\sigma_+\sigma_-\rangle_{ss})^{-1} \approx \tau_{av}$, but $w_{ss}(\tau)$ decays to zero for $\tau > \tau_{av}$ as it becomes more and more unlikely that the *next* photopulse has not yet arrived.

Note 2.9 Equation (2.156) can be derived by considering a random sequence of photopulses, with a probability $\eta'\gamma\langle\sigma_+\sigma_-\rangle_{ss}\Delta t$ for finding a photopulse in any short interval Δt and a probability $1-\eta'\gamma\langle\sigma_+\sigma_-\rangle_{ss}\Delta t$ for not finding a photopulse in the same interval. The probability for finding no photopulses throughout an interval $\tau = m\Delta t$, and then finding a photopulse in the interval from τ to $\tau+\Delta t$, is just

$$\begin{aligned}
&\eta'\gamma\langle\sigma_+\sigma_-\rangle_{ss}\Delta t\big(1-\eta'\gamma\langle\sigma_+\sigma_-\rangle_{ss}\Delta t\big)^m \\
&\quad=\eta'\gamma\langle\sigma_+\sigma_-\rangle_{ss}\Delta t\sum_{n=0}^{m}\frac{m!}{(m-n)!n!}\big(-\eta'\gamma\langle\sigma_+\sigma_-\rangle_{ss}\Delta t\big)^n \\
&\quad=\eta'\gamma\langle\sigma_+\sigma_-\rangle_{ss}\Delta t\sum_{n=0}^{m}m(m-1)\cdots(m-n+1) \\
&\qquad\times\frac{\big(-\eta'\gamma\langle\sigma_+\sigma_-\rangle_{ss}\Delta t\big)^n}{n!} \\
&\quad=\eta'\gamma\langle\sigma_+\sigma_-\rangle_{ss}\Delta t\sum_{n=0}^{m}\Big(1-\frac{1}{m}\Big)\Big(1-\frac{2}{m}\Big)\cdots\Big(1-\frac{n-1}{m}\Big) \\
&\qquad\times\frac{\big(-\eta'\gamma\langle\sigma_+\sigma_-\rangle_{ss}\Delta t\big)^n}{n!}.
\end{aligned}$$

On taking the limit $m\to\infty$, $\Delta t\to 0$, with $m\Delta t=\tau$, this gives

$$w_{ss}(\tau)dt=\eta'\gamma\langle\sigma_+\sigma_-\rangle_{ss}dt\exp\big(-\eta'\gamma\langle\sigma_+\sigma_-\rangle_{ss}\tau\big).$$

Now, in what sense does (2.153) imply an "antibunching" of photopulses? Figure 2.7 illustrates the behavior of $w_{ss}(\tau)$ for the light scattered in resonance fluorescence compared with coherent light of the same intensity. There is unit area under both of the curves plotted in the figure [Eq. (2.154)], and both distributions give the same mean time τ_{av} between photopulses. Note, now, that we have the equivalence

$$g^{(2)}_{ss}(0)<1 \iff w_{ss}(0)=(\eta'\gamma\langle\sigma_+\sigma_-\rangle_{ss})g^{(2)}_{ss}(0)<\eta'\gamma\langle\sigma_+\sigma_-\rangle_{ss}.$$

Thus, (2.153) guarantees that $w_{ss}(0)$ falls below its value for coherent light of the same intensity. Then with increasing τ, $w_{ss}(\tau)$ must first rise above the

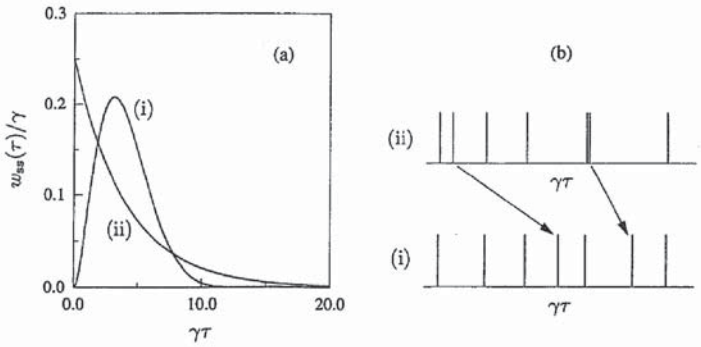

Fig. 2.7 (a) Waiting-time distribution for resonance fluorescence [curve (i)] and coherent scattering of the same intensity [curve (ii)], for $Y^2=1$, and $\eta'=1$. (b) Rearrangement of a typical random photopulse sequence to account for the change in the waiting-time distribution shown in (a).

exponential curve for coherent light, ensuring that both distributions have unit area, and then fall below it once again to ensure that both distributions give the same τ_{av}. We conclude that in comparison with coherent light of the same intensity, on the average, photopulse sequences are redistributed as illustrated in Fig. 2.7: some photopulses are moved from positions where they separate two very short time intervals, to new positions where they divide some of the very long time intervals into two. The result, as displayed in Fig. 2.7, is that the very shortest and very longest intervals between photopulses become less likely, and the intervals of intermediate length become more likely. A move is made away from photopulse sequences showing bunches and gaps, towards more regimented, evenly spaced, sequences.

Exercise 2.6 For perfect collection and detection efficiencies ($\eta'=1$) $w_{ss}(\tau)$ can be calculated from [2.50, 2.51]

$$w_{ss}(\tau)=\langle 2|\bar{\rho}(\tau)|2\rangle_{\rho(0)=|1\rangle\langle 1|}=\langle 2|e^{\bar{\mathcal{L}}\tau}\big(|1\rangle\langle 1|\big)|2\rangle,$$

where the action of the superoperator $\bar{\mathcal{L}}$ on an operator $\hat{O}$ is given by

$$\bar{\mathcal{L}}\hat{O}\equiv\mathcal{L}\hat{O}-\gamma\sigma_-\hat{O}\sigma_+,$$

with $\mathcal{L}$ defined by the right-hand-side of (2.96). For these conditions show that the *photoelectron waiting-time distribution of resonance fluorescence at unit detection efficiency* is given by

$$w_{ss}(\tau)=\gamma e^{-(\gamma/2)\tau}\frac{Y^2}{2Y^2-1}(1-\cosh\delta'\tau), \tag{2.158}$$

with

$$\delta' \equiv \frac{\gamma}{2}\sqrt{1-2Y^2}. \tag{2.159}$$

Verify that (2.154) is satisfied and that the mean interval between photopulses is $\tau_{\rm av} = \gamma^{-1}2(1+Y^2)/Y^2 = \left(\gamma\langle\sigma_+\sigma_-\rangle_{\rm ss}\right)^{-1} =$ (photon emission rate)$^{-1}$. Plot $w_{\rm ss}(\tau)$ for $2Y^2 = 1$ and compare it with the exponential $w_{\rm ss}(\tau) = (\gamma/6)\exp[-(\gamma/6)\tau]$ obtained for coherent light of the same intensity.

The central feature of this definition of photon antibunching is that it is made *in comparison with coherent light of the same intensity*. An alternative definition adopted by Mandel and co-workers [2.48, 2.49] does not make such a comparison. In addition to satisfying (2.153), the curves of Fig 2.6 also have

$$g^{(2)\prime}_{\rm ss}(0) = 0, \qquad g^{(2)\prime\prime}_{\rm ss}(0) > 0; \tag{2.160}$$

the prime denotes differentiation with respect to τ. Classically, $g^{(2)}_{\rm ss}(\tau)$ must decrease from its value at $\tau = 0$, or, of course, remain constant if the light is coherent. Stated in terms of $w_{\rm ss}(\tau)$, no interval between photopulses may be more probable than $\tau = 0$. Mandel and co-workers identify photon antibunching with an initially rising $g^{(2)}_{\rm ss}(\tau)$. Since the most probable interval between photopulses is then some $\tau \neq 0$, photopulse sequences show a dirth of "tight" bunches in favor of somewhat larger photopulse separations, giving alternative definition to the term "antibunched."

This concept is drawn entirely from a comparison made within the photopulse sequences for the antibunched light – there are more slightly longer photopulse separation times than there are very short separation times. No comparison is made against the reference of coherent light of the same intensity. It is actually possible for photopulse sequences to be bunched in the sense of our previous discussion – with increased probability for short and long photopulse separation times and decreased probability for intermediate separation times – and be antibunched according to this second definition. This possibility is illustrated by Fig. 2.8. The converse also occurs, with (2.153) satisfied and $g^{(2)}_{\rm ss}(\tau)$ initially decreasing. Such behavior is seen in the forwards fluorescence from a single atom inside a resonant optical cavity [2.53].

The use of two definitions for photon antibunching might be a little confusing; but it is not really a major problem. Both definitions identify nonclassical effects. We must remember, however, that strictly these are *distinct* nonclassical effects. Both effects have been demonstrated in experiments on resonance fluorescence [2.33, 2.48, 2.49]. Of course, whenever $g^{(2)}_{\rm ss}(0) = 0$ [as in (2.152)], the two definitions will be satisfied together. For definiteness we will use "photon antibunching" in the sense of (2.153), which seems to be more in accord with the traditional interpretation of the photon bunching of Hanbury-Brown and Twiss.

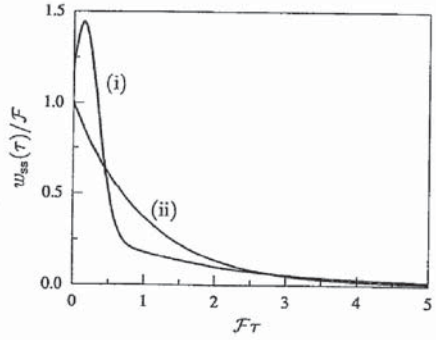

Fig. 2.8 Waiting-time distribution for light that is bunched in the sense of the discussion below (2.153) and antibunched according to the definition (2.160) [curve (i)]. An example of this behavior is shown in Ref. [2.52], Fig. 11(c). $\mathcal{F}$ is the mean photon flux and curve (ii) is the waiting-time distribution for coherent light.

Note 2.10 The definition of photon antibunching given by (2.153) is equivalent to the condition for sub-Poissonian photon counting statistics for short counting times. A single-mode field illustrates this point:

$$\begin{aligned} g^{(2)}(0) &= \langle a^\dagger a\rangle^{-2}\langle a^{\dagger 2}a^2\rangle \\ &= \langle a^\dagger a\rangle^{-2}\left[\langle(a^\dagger a)^2\rangle - \langle a^\dagger a\rangle\right] \\ &= 1 + \frac{\left(\langle\hat{n}^2\rangle - \langle\hat{n}\rangle^2\right) - \langle\hat{n}\rangle}{\langle\hat{n}\rangle^2}, \end{aligned}$$

where $\hat{n} \equiv a^\dagger a$ is the photon number operator. Then

$$g^{(2)}(0) - 1 = \frac{Q}{\langle\hat{n}\rangle}, \tag{2.161}$$

where the *Mandel Q parameter*,

$$\begin{aligned} Q &\equiv \frac{\left(\langle\hat{n}^2\rangle - \langle\hat{n}\rangle^2\right) - \langle\hat{n}\rangle}{\langle\hat{n}\rangle} \\ &= \frac{\langle(\Delta\hat{n})^2\rangle - \langle\hat{n}\rangle}{\langle\hat{n}\rangle}, \end{aligned} \tag{2.162}$$

measures the departure from Poissonian statistics. Clearly, (2.153) is equivalent to the condition for sub-Poissonian statistics, $Q < 1$. On the other hand, when counting times are not short on the scale of the field correlation time, the definition of Q involves integrals over field correlation functions; then (2.153) is no longer equivalent to the condition $Q < 1$.

Before we leave our discussion of photon antibunching, now is a good time to introduce some of the ideas concerning "squeezed" states of the electromagnetic field [2.54]. Walls and Zoller [2.55] pointed out that the light scattered in resonance fluorescence is squeezed in the field quadrature that is in phase with the mean scattered field amplitude. This squeezing is closely related to photon antibunching. We do not want to make a diversion into a detailed discussion of squeezed states here, and anyone who is totally unfamiliar with the subject may find it helpful to refer to the introductory article by Walls [2.56]. We will return to the subject of squeezing in Volume II (Chap. 9) and the discussion of background material is postponed until then.

When we write

$$g^{(2)}_{ss}(0) = \left(\langle\sigma_+\sigma_-\rangle_{ss}\right)^{-2}\langle\sigma_+^2\sigma_-^2\rangle_{ss} \tag{2.163}$$

it is quite obvious that $g^{(2)}_{ss}(0)$ vanishes; we have discussed the simple reason for this above. There is something more to be learned, however, if we look at (2.163) in a slightly different way [2.57]. We may always regard the scattered field as the sum of a coherent component $\langle\hat{E}_s^{(+)}\rangle_{ss}$, which is proportional to $\langle\sigma_-\rangle_{ss}$, and a fluctuating component described by the operator $\Delta\hat{E}_s^{(+)} = \hat{E}_s^{(+)} - \langle\hat{E}_s^{(+)}\rangle_{ss}$, which is proportional to $\Delta\sigma_- = \sigma_- - \langle\sigma_-\rangle_{ss}$. Looked at in this way, (2.163) may be expanded along the same lines as the fluorescence spectrum [Eqs. (2.122)–(2.126)]; after transforming to a rotating frame, we may write

$$\begin{aligned} g^{(2)}_{ss}(0) - 1 = \left(A^2 + \langle\Delta\tilde{\sigma}_+\Delta\tilde{\sigma}_-\rangle_{ss}\right)^{-2}\Big[&A^2 4\langle : \Delta\tilde{\sigma}_{\frac{\pi}{2}})^2 : \rangle_{ss} \\ &+ 4A\mathrm{Re}\left(e^{i\frac{\pi}{2}}\langle(\Delta\tilde{\sigma}_+)^2\Delta\tilde{\sigma}_-\rangle_{ss}\right) + \langle(\Delta\tilde{\sigma}_+)^2(\Delta\tilde{\sigma}_-)^2\rangle_{ss} \\ &- \left(\langle\Delta\tilde{\sigma}_+\Delta\tilde{\sigma}_-\rangle_{ss}\right)^2\Big], \end{aligned} \tag{2.164}$$

where $\langle\ :\ :\ \rangle$ denotes the normal-ordered average (with $\Delta\tilde{\sigma}_+$ to the left of $\Delta\tilde{\sigma}_-$); using (2.120a), we have defined

$$A \equiv |\langle\tilde{\sigma}_{\mp}\rangle_{ss}| = \frac{1}{\sqrt{2}}\frac{Y}{1+Y^2}, \tag{2.165}$$

and

$$\Delta\tilde{\sigma}_{\frac{\pi}{2}} \equiv \tfrac{1}{2}\left(e^{-i\frac{\pi}{2}}\Delta\tilde{\sigma}_- + e^{i\frac{\pi}{2}}\Delta\tilde{\sigma}_+\right) \tag{2.166}$$

describes fluctuations in the quadrature of the scattered field that is in phase with the mean scattered field amplitude. What is to be gained from this decomposition? To answer this question we must first calculate the steady-state correlations that appear in (2.164):

Exercise 2.7 Show that

$$\langle\Delta\tilde{\sigma}_+\Delta\tilde{\sigma}_-\rangle_{ss} = \frac{1}{2}\frac{Y^4}{(1+Y^2)^2}, \tag{2.167a}$$

$$\langle : (\Delta\tilde{\sigma}_{\frac{\pi}{2}})^2 : \rangle_{ss} = \frac{1}{4}\frac{Y^2(Y^2-1)}{(1+Y^2)^2}, \tag{2.167b}$$

$$2\mathrm{Re}\left(e^{i\frac{\pi}{2}}\langle(\Delta\tilde{\sigma}_+)^2\Delta\tilde{\sigma}_-\rangle_{ss}\right) = \sqrt{2}\frac{Y^5}{(1+Y^2)^3}, \tag{2.167c}$$

$$\langle(\Delta\tilde{\sigma}_+)^2(\Delta\tilde{\sigma}_-)^2\rangle_{ss} - \left(\langle\Delta\tilde{\sigma}_+\Delta\tilde{\sigma}_-\rangle_{ss}\right)^2 = \frac{1}{4}\frac{Y^4(1+4Y^2-Y^4)}{(1+Y^2)^4}. \tag{2.167}$$

Now, when (2.165) and (2.167a)–(2.167d) are substituted into (2.164), the answer $g^{(2)}_{ss}(0) = 0$ must, of course, be recovered for all field strengths Y. The relative importance of the terms within the square bracket changes with Y, however, and it is here that the new insight lies. For weak fields ($Y^2 << 1$), the dominant terms in (2.164) are

$$A^2 + \langle\Delta\tilde{\sigma}_+\Delta\tilde{\sigma}_-\rangle_{ss} \approx A^2 \approx \tfrac{1}{2}Y^2, \tag{2.168a}$$

$$A^2 4\langle : (\Delta\tilde{\sigma}_{\pi/2})^2 : \rangle_{ss} \approx -\tfrac{1}{2}Y^4, \tag{2.168b}$$

$$\langle(\Delta\tilde{\sigma}_+)^2(\Delta\tilde{\sigma}_-)^2\rangle_{ss} - \left(\langle\Delta\tilde{\sigma}_+\Delta\tilde{\sigma}_-\rangle_{ss}\right)^2 \approx \tfrac{1}{4}Y^4. \tag{2.168c}$$

For strong fields ($Y^2 >> 1$) they are

$$A^2 + \langle\Delta\tilde{\sigma}_+\Delta\tilde{\sigma}_-\rangle_{ss} \approx \langle\Delta\tilde{\sigma}_+\Delta\tilde{\sigma}_-\rangle_{ss} \approx \tfrac{1}{4}, \tag{2.169a}$$

$$\langle(\Delta\tilde{\sigma}_+)^2(\Delta\tilde{\sigma}_-)^2\rangle_{ss} - \left(\langle\Delta\tilde{\sigma}_+\Delta\tilde{\sigma}_-\rangle_{ss}\right)^2 \approx -\tfrac{1}{4}. \tag{2.169b}$$

Observe that the negative term, which is the source of the antibunching – it will produce the -1 on the left-hand side of (2.164) [remember that the $g^{(2)}_{ss}(0)$ on the left-hand side is zero] – comes from the first term inside the square bracket on the right-hand side of (2.164) for weak fields, and from the third term inside the square bracket for strong fields. These terms, respectively, describe self-homodyning between the incoherent and coherent components of the scattered field, and intensity fluctuations in the incoherent component of the scattered field. Thus, a different physical picture for the fluctuations in the antibunched field is suggested in the weak-field and strong-field limits. A negative value for $\langle : (\Delta\tilde{\sigma}_{\pi/2})^2 : \rangle_{ss}$ is the signature of squeezing; thus, at weak fields photon antibunching arises from the *self-homodyning of squeezed fluorescence*; here photon antibunching is associated with the nonclassical statistics of a *phased* oscillator. Phase information is destroyed in the strong-field limit. For strong excitation the coherent component of the scattered field saturates and the homodyning term in (2.164) becomes unimportant. Photon antibunching in the strong-field limit arises from sub-Poissonian intensity fluctuations in an *unphased* scattered field. For a suggestive illustration we can compare a displaced squeezed vacuum state (weak fields) and a one-photon Fock state (strong fields), as illustrated by Fig. 2.9.

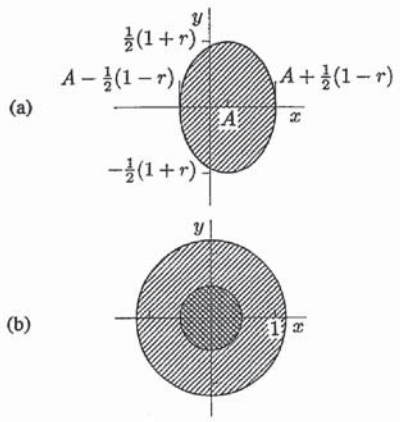

Fig. 2.9 Schematic illustration of the fluctuations in the two quadrature phase amplitudes of (a) a displaced weakly squeezed vacuum state (squeeze parameter $r = A^2$) and (b) a one-photon Fock state. Both states have $g^{(2)}(0) = 0$ (to lowest order in A^2 for the squeezed state). The curves are contours of the Wigner distribution (see Chap. 4).

Note 2.11 One scheme for detecting squeezing, described by Mandel [2.58], involves homodyning the scattered light with a strong local oscillator and measuring photon-counting statistics as a function of the local oscillator phase. Squeezing is indicated by a phase dependent variation from super-Poissonian statistics, when the unsqueezed quadrature is selected by the local oscillator phase, to sub-Poissonian statistics, when the squeezed quadrature is selected by the local oscillator phase. Equation (2.164) corresponds to a special case of this procedure where the local oscillator is the coherent fluorescent scattering itself. Under these conditions we do not, of course, have control over the local oscillator amplitude and phase. To convert the expressions we have derived so that they describe a squeezing measurement for the fluorescence in accord with Mandel's scheme we simply replace A by a large local oscillator amplitude B, and replace $\frac{\pi}{2}$ by an adjustable phase ϕ. If the local oscillator intensity is much larger than the fluorescence intensity, the combined field of local oscillator plus fluorescent scattering then gives

$$g^{(2)}_{ss}(0) - 1 \approx \frac{4\langle :(\Delta\tilde{\sigma}_\phi)^2: \rangle_{ss}}{B^2}. \tag{2.170}$$

Actually, B is not the local oscillator field amplitude, it is only proportional to this amplitude. The proportionality is the same as that between σ_- and $\hat{E}_s^{(+)}$; from (2.138), it is such that the mean number of photons counted during ΔT, for a detection efficiency η and solid angle $\Delta\Omega$, is

$$\langle\hat{n}\rangle = \eta\gamma\Delta T\frac{\Delta\Omega\sin^2\theta}{8\pi/3}B^2. \tag{2.171}$$

Substituting from (2.170) and (2.171) into (2.161), the photon counting distribution is characterized, as either super-Poissonian or sub-Poissonian, by

$$Q_\phi = \eta\gamma\Delta T\frac{\Delta\Omega\sin^2\theta}{8\pi/3}4\langle :(\Delta\tilde{\sigma}_\phi)^2: \rangle_{ss}. \tag{2.172}$$

When the oscillator phase is $\frac{\pi}{2}$,

$$Q_{\frac{\pi}{2}} = \eta\gamma\Delta T\frac{\Delta\Omega\sin^2\theta}{8\pi/3}\frac{Y^2(Y^2-1)}{(1+Y^2)^2}. \tag{2.173}$$

This gives sub-Poissonian counting statistics for $Y^2 < 1$. An explicit expression for arbitrary ϕ can be calculated as an exercise.